Hourglass Arrays, and Other Novel 2D Sparse Arrays with Reduced Mutual Coupling

Chun-Lin Liu, *Student Member, IEEE,* and P. P. Vaidyanathan, *Fellow, IEEE*

Abstract

Linear (1D) sparse arrays such as nested arrays and minimum redundancy arrays have hole-free difference coarrays with $O(N^2)$ virtual sensor elements, where N is the number of physical sensors. The hole-free property makes it easier to perform beamforming and DOA estimation in the coarray domain which behaves like an uniform linear array. The $O(N^2)$ property implies that $O(N^2)$ uncorrelated sources can be identified. For the 2D case, planar sparse arrays with hole-free coarrays having $O(N^2)$ elements have also been known for a long time. These include billboard arrays, open box arrays (OBA), and 2D nested arrays. Their merits are similar to those of the 1D sparse arrays mentioned above, although identifiability claims regarding $O(N^2)$ sources have to be handled with more care in 2D. This paper introduces new planar sparse arrays with hole-free coarrays having $O(N^2)$ elements just like the OBA, with the additional property that the number of sensor pairs with small spacings such as $\lambda/2$ decreases, reducing the effect of mutual coupling. The new arrays include half open box arrays (HOBA), half open box arrays with two layers (HOBA-2), and hourglass arrays. Among these, simulations show that hourglass arrays have the best estimation performance in presence of mutual coupling.

Index Terms

Nonseparable 2D sparse arrays, open box arrays, hourglass arrays, mutual coupling, DOA estimation.

I. Introduction

Planar (2D) arrays find useful applications in beamforming, radar, imaging, and communications [2]–[4]. They can jointly estimate the azimuth and elevation of sources [2]. Some well-known 2D array geometries include uniform rectangular arrays (URA), uniform circular arrays (UCA), and hexangonal arrays, in which elements are placed uniformly on regular contours [2]. However, these array configurations usually suffer from significant mutual coupling, resulting in considerable interferences between sensor outputs [5], [6].

It is well-known that large sensor separations help to reduce the mutual coupling effect [5], [6]. Hence, linear (1D) *sparse arrays*, in which the number of sensor pairs with small separations is much smaller than in uniform linear arrays (ULA), are more robust to mutual coupling [7]. Examples of linear sparse arrays include minimum

This work was supported in parts by the ONR grant N00014-15-1-2118, the California Institute of Technology, and the Taiwan/Caltech Ministry of Education Fellowship. Part of the results was presented at the Asilomar Conference on Signals, Systems, and Computers, Pacific Grove, CA, USA, Nov. 2016 [1].

The authors are with the California Institute of Technology, Pasadena, CA 91125, USA (e-mail: cl.liu@caltech.edu; ppvnath@systems.caltech.edu).

(a) (b)

Fig. 1. The array geometry of (a) open box arrays (OBA) and (b) hourglass arrays, in units of half of the wavelength ($\lambda/2$). Definition 3 and 8 give the formal description. The parameters are $N_x = 13$ and $N_y = 19$. Red and blue bullets represent physical sensors while crosses denote empty space.

redundancy arrays (MRA) [8], nested arrays [9], coprime arrays [10], super nested arrays [7], [11], and other generalizations [12]–[14]. Among these, super nested arrays and coprime arrays are significantly robust to mutual coupling effects because they have very few sensor pairs with small separations. Super nested arrays have an additional advantage over coprime arrays because the coarrays are filled (*hole-free*). Unlike MRAs which share the hole-free property, the sensor locations in a super nested array also have a simple closed form.

Planar arrays with hole-free difference coarrays (that is, coarrays that are URAs), are important for several reasons. First, if the coarrays have $O(N^2)$ elements, then $O(N^2)$ uncorrelated DOAs can be identified under some restrictions on the DOA locations [15][1]. Second, there is evidence from the literature on 2D arrays [17], [18] that sparse arrays with hole-free coarrays produce better responses in beamforming applications. Finally, when DOA estimation algorithms such as MUSIC and ESPRIT are used directly on the sparse array, they do not work well, as they create ambiguities [19], [20]. However, if these algorithms are used on the ULA or URA part of the coarray domain (e.g., using spatial smoothing), they work very well [9], [10], [13]–[15], [21], [22]. For these reasons, we focus on the design of 2D sparse arrays with coarrays which are URAs with $O(N^2)$ elements.

For 2D arrays, it is desirable to have closed-form sensor locations, large and hole-free difference coarrays, and less mutual coupling, like 1D super nested arrays. However, such 2D arrays are not fully explored in the literature. Some existing designs enjoy closed-form sensor locations with hole-free coarrays, including billboard arrays, 2D nested arrays, and open box arrays (OBA) [17], [18], [23], [24]. Hence, inspired by [16], one can expect that these 2D sparse arrays could distinguish more sources than sensors almost surely. Nevertheless, none of them takes the mutual coupling issue into account.

In this paper, we will develop some new 2D sparse arrays that decrease mutual coupling effects in OBA. These novel array configurations include *half open box arrays (HOBA)*, *half open box arrays with two layers (HOBA-2)*,

[1]For arbitrary source locations, the $O(N^2)$ result is not as strong as in the 1D case because, identifiability in 2D can only be guaranteed in an almost sure sense [16].

and *hourglass arrays*. By redistributing the sensors in OBA systematically, these arrays are guaranteed to have the same number of sensors as OBA, and to possess hole-free coarrays with enhanced degrees of freedom (Theorem 1, 2, 3, and 4), which makes it possible to detect more sources than sensors. Moreover, it will be shown that the number of sensor pairs with small spacing ($\lambda/2$ and $\sqrt{2}\lambda/2$) decreases considerably (Table I), indicating that mutual coupling effect decreases significantly.

Fig. 1 offers a first glance of (a) OBA and (b) hourglass arrays. The array geometry for OBA resembles the side view of a box with an open top. The sensor locations for hourglass arrays resemble an hourglass with two pillars on both sides. The closed-form sensor locations for these arrays will be shown in Defintion 3 and 8, respectively.

In this example, it can be shown that both arrays have 49 physical sensors and hole-free coarrays. However, in OBA, there are 12 sensor pairs with separation $(\lambda/2, 0)$ and 36 pairs with separation $(0, \lambda/2)$. On the other hand, in hourglass arrays, there are only 2 sensor pairs with separation $(\lambda/2, 0)$ and 8 pairs with spacing $(0, \lambda/2)$, which are much smaller than those in OBA. This property makes hourglass arrays more robust to mutual coupling effects, as demonstrated in Section VIII. All these properties will be given in depth later.

This paper is outlined as follows. Section II reviews the data model and several well-known 2D arrays, like URA, billboard arrays, 2D nested arrays, and OBA. In Section III, the horizontal segment in OBA is generalized into partially open box arrays (POBA) and half open box arrays (HOBA). Section IV extends POBA to POBA with L layers (POBA-L) by designing the vertical segments in POBA properly. Section V and VI propose HOBA with two layers (HOBA-2), and hourglass arrays, respectively, based on the theory developed in Section IV. For all these 2D arrays, the expression for the weight functions with small separations are listed in Section VII with detailed derivation. Section VIII demonstrates the superior performance of the proposed arrays in the presence of mutual coupling while Section IX concludes this paper.

For the reader's convenience, [25] provides a MATLAB function `POBA_L.m`, which takes some descriptive parameters of the array as inputs and returns the sensor locations as outputs. Furthermore, `interactive_interface.m` offers an interactive panel where users can readily design their array geometries and visualize the weight functions.

II. Preliminaries

A. The Data Model

Suppose D uncorrelated sources impinge on a 2D array, whose sensors are located at $\mathbf{n}d$. Here $\mathbf{n} = (n_x, n_y) \in \mathbb{Z}^2$ is an integer-valued vector and $d = \lambda/2$ is the minimum separation between sensors. The sensor locations $\mathbf{n}$ form a set $\mathbb{S}$. The ith source has complex amplitude $A_i \in \mathbb{C}$, azimuth $\phi_i \in [0, 2\pi]$, and elevation $\theta_i \in [0, \pi]$. If mutual coupling is absent, the sensor output on $\mathbb{S}$ can be modeled as

$$\mathbf{x}_{\mathbb{S}} = \sum_{i=1}^{D} A_i \mathbf{v}_{\mathbb{S}}(\bar{\theta}_i, \bar{\phi}_i) + \mathbf{n}_{\mathbb{S}}, \tag{1}$$

where $\bar{\theta}_i = (d/\lambda)\sin\theta_i\cos\phi_i$ and $\bar{\phi}_i = (d/\lambda)\sin\theta_i\sin\phi_i$ are the normalized DOA. The element of the steering vector $\mathbf{v}_{\mathbb{S}}(\bar{\theta}_i, \bar{\phi}_i)$ corresponding to the sensor at $(n_x, n_y) \in \mathbb{S}$ is $e^{j2\pi(\bar{\theta}_i n_x + \bar{\phi}_i n_y)}$. Signals and noise are assumed to be zero-mean and uncorrelated. That is, $\mathbb{E}[A_i] = 0, \mathbb{E}[\mathbf{n}_{\mathbb{S}}] = \mathbf{0}, \mathbb{E}[A_i A_j^*] = \sigma_i^2 \delta_{i,j}, \mathbb{E}[\mathbf{n}_{\mathbb{S}} \mathbf{n}_{\mathbb{S}}^H] = \sigma^2 \mathbf{I}, \mathbb{E}[A_i \mathbf{n}_{\mathbb{S}}^H] = \mathbf{0}$, where σ_i^2 and σ^2 are the ith source power and the noise power, respectively. $\delta_{p,q}$ is the Kronecker delta.

For uncorrelated sources, the covariance matrix of $\mathbf{x}_\mathbb{S}$ can be expressed as

$$\mathbf{R}_\mathbb{S} = \mathbb{E}[\mathbf{x}_\mathbb{S}\mathbf{x}_\mathbb{S}^H] = \sum_{i=1}^{D} \sigma_i^2 \mathbf{v}_\mathbb{S}(\bar{\theta}_i, \bar{\phi}_i)\mathbf{v}_\mathbb{S}^H(\bar{\theta}_i, \bar{\phi}_i) + \sigma^2\mathbf{I}. \tag{2}$$

Vectorizing (2) and removing duplicated entries yield the signal on the difference coarray [9], [21], [26], [27]:

$$\mathbf{x}_\mathbb{D} = \sum_{i=1}^{D} \sigma_i^2 \mathbf{v}_\mathbb{D}(\bar{\theta}_i, \bar{\phi}_i) + \sigma^2\mathbf{e}_0, \tag{3}$$

where $\mathbf{e}_0$ is a column vector with $\langle \mathbf{e}_0 \rangle_{(n_x,n_y)} = \delta_{n_x,0}\delta_{n_y,0}$. The bracket notation $\langle \mathbf{x}_\mathbb{S} \rangle_\mathbf{n}$ [27] denotes the value of the signal at the support location $\mathbf{n} \in \mathbb{S}$. For instance, if $\mathbb{S} = \{(0,0),(1,0),(0,1)\}$ and $\mathbf{x}_\mathbb{S} = [4,5,6]^T$, then $\langle \mathbf{x}_\mathbb{S} \rangle_{(0,0)} = 4$, $\langle \mathbf{x}_\mathbb{S} \rangle_{(1,0)} = 5$, and $\langle \mathbf{x}_\mathbb{S} \rangle_{(0,1)} = 6$. $\mathbb{D}$ is the difference coarray, which is defined as

Definition 1 (Difference coarray): For a 2D array specified by $\mathbb{S}$, its difference coarray $\mathbb{D}$ is defined as the differences between sensor locations:

$$\mathbb{D} = \{\mathbf{n}_1 - \mathbf{n}_2 \mid \mathbf{n}_1, \mathbf{n}_2 \in \mathbb{S}\}.$$

For example, if $\mathbb{S}$ consists of $(0,0)$, $(1,0)$, $(2,0)$, $(0,1)$, $(2,1)$, $(0,2)$, $(2,2)$, then the difference coarray $\mathbb{D}$ is composed of integer vectors (m_x, m_y) such that $-2 \leq m_x, m_y \leq 2$. The uniform rectangular part of $\mathbb{D}$ is denoted by $\mathbb{U}$. In this example, $\mathbb{D} = \mathbb{U}$, and such array is said to have a *hole-free coarray*. More generally, if the coarray is the set of all integer vectors within a parallelepiped, we can regard it as hole-free, but we shall not consider this extension here.

If mutual coupling is present, the data model (1) becomes

$$\mathbf{x}_\mathbb{S} = \sum_{i=1}^{D} A_i \mathbf{C}\mathbf{v}_\mathbb{S}(\bar{\theta}_i, \bar{\phi}_i) + \mathbf{n}_\mathbb{S}, \tag{4}$$

where $\mathbf{C}$ is the mutual coupling matrix [5], [28]–[30]. In this paper, we assume that the entries of $\mathbf{C}$ can be characterized by [5]

$$\langle \mathbf{C} \rangle_{\mathbf{n}_1,\mathbf{n}_2} = \begin{cases} c(\|\mathbf{n}_1 - \mathbf{n}_2\|_2), & \text{if } \|\mathbf{n}_1 - \mathbf{n}_2\|_2 \leq B, \\ 0 & \text{otherwise}, \end{cases} \tag{5}$$

where $\mathbf{n}_1, \mathbf{n}_2 \in \mathbb{S}$ denote the sensor locations. Here $\|\cdot\|_2$ is the ℓ_2-norm of a vector and $c(\cdot)$ are the mutual coupling coefficients. It is assumed that $c(0) = 1$ and $|c(k)/c(\ell)| = \ell/k$ for $k, \ell > 0$ [5], implying that the arrays with larger sensor separations, like sparse arrays, tend to reduce mutual coupling. To quantify mutual coupling, we first define the weight function:

Definition 2 (Weight function): Let a 2D array be specified by $\mathbb{S}$, and let its difference coarray be $\mathbb{D}$. The weight function $w(\mathbf{m})$ is the number of pairs with separation $\mathbf{m} \in \mathbb{D}$, i.e.,

$$w(\mathbf{m}) = \left|\{(\mathbf{n}_1, \mathbf{n}_2) \in \mathbb{S}^2 \mid \mathbf{n}_1 - \mathbf{n}_2 = \mathbf{m}\}\right|.$$

We will use $w(\mathbf{m})$ and $w(m_x, m_y)$ interchangeably, where $\mathbf{m} = (m_x, m_y)$. It was shown in [7] that, qualitatively, smaller weight functions at small sensor separations reduce the effect of mutual coupling significantly.

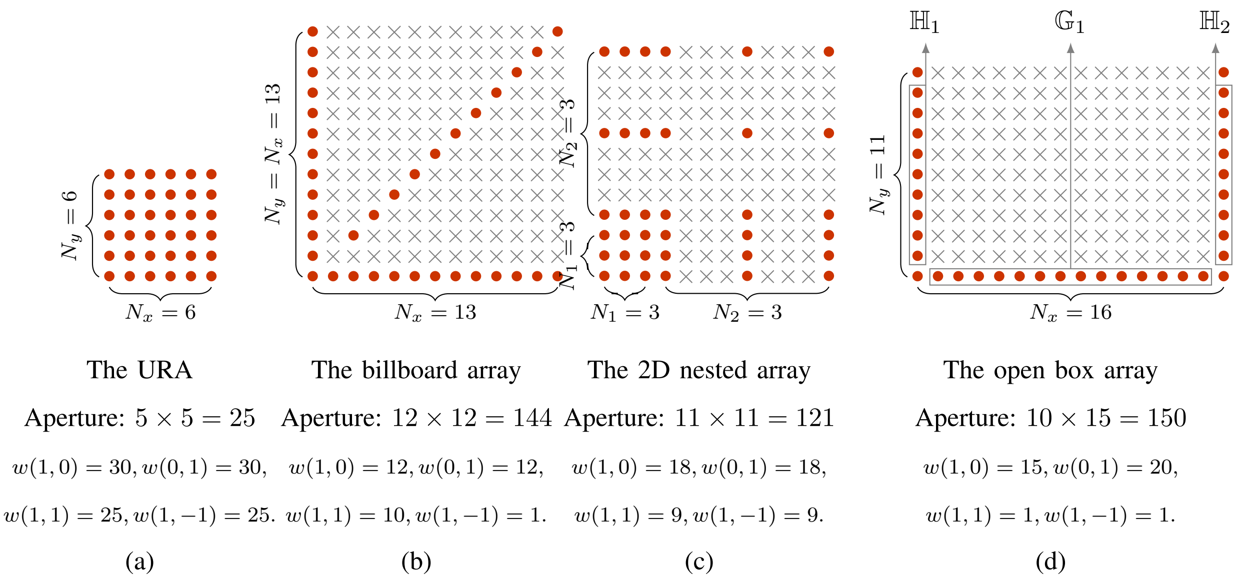

Fig. 2. Examples of 2D arrays with $N = 36$ elements. Bullets denote physical sensors and crosses represent empty space. The minimum separation between sensors is $\lambda/2$.

B. Known Closed-Form 2D Sparse Arrays

In this subsection, we will review some known 2D arrays on rectangular grids with regular geometries, in Fig. 2.

The URA places $N_x N_y$ sensors on an N_y-by-N_x rectangular grid, as demonstrated in Fig. 2(a) for 36 sensors. The billboard array [23] consists of three ULA on a square aperture ($N_x = N_y$) and the total number of sensors is $3(N_x - 1)$, as in Fig. 2(b). The 2D nested array [24] is depicted in Fig. 2(c). In this example, this array is the cross product of two identical 1D nested arrays with $N_1 = N_2 = 3$ (notation as in [9]) and the number of sensors is $(N_1 + N_2)^2$. Finally, the open box array [17] assigns $N_x + 2N_y - 2$ sensors on the boundaries of a rectangular aperture, as illustrated in Fig. 2(d). The definition of OBA is also given by[2]

Definition 3 (Open box arrays, OBA): Let N_x and N_y be positive integers. An open box array is characterized by the integer set $\mathbb{S}_{\text{OBA}}$, defined by

$$\begin{aligned}\mathbb{S}_{\text{OBA}} = &\{(0,0),\ (N_x-1,0),\ (0,N_y-1),\ (N_x-1,N_y-1)\}\\ &\cup \mathbb{G}_1 \cup \mathbb{H}_1 \cup \mathbb{H}_2,\end{aligned}$$

where $\mathbb{G}_1 = \{(n_x, 0) \mid n_x \in \mathfrak{g}_1\}$, $\mathbb{H}_1 = \{(0, n_y) \mid n_y \in \mathfrak{h}_1\}$, and $\mathbb{H}_2 = \{(N_x - 1, n_y) \mid n_y \in \mathfrak{h}_2\}$. Here $\mathfrak{g}_1 = \{1, 2, \ldots, N_x - 2\}$ and $\mathfrak{h}_1 = \mathfrak{h}_2 = \{1, 2, \ldots, N_y - 2\}$.

[2]In this paper, the sensor locations are defined formally, as in Definition 3. This helps to develop novel array configurations systematically and to compute the sensor locations readily [25].

Fig. 2(d) marks the sets $\mathbb{G}_1$, $\mathbb{H}_1$, and $\mathbb{H}_2$ in rectangles on the bottom, on the left, and on the right, respectively. Furthermore, the difference coarray of OBA is given as

$$\mathbb{D}_{\text{OBA}} = \{(m_x, m_y) \in \mathbb{Z}^2 \mid -N_x + 1 \leq m_x \leq N_x - 1, \\ -N_y + 1 \leq m_y \leq N_y - 1\}, \tag{6}$$

which is exactly a uniform rectangular region.

All of the arrays in Fig. 2 have 36 physical sensors and hole-free coarrays ($\mathbb{D} = \mathbb{U}$). However, the sizes of difference coarrays are different. The largest $|\mathbb{D}|$ is exhibited by the OBA (651), followed by the billboard array (625), the 2D nested array (529), and finally the URA (121). Empirically, larger $|\mathbb{D}|$ is more likely to offer better spatial resolution and more resolvable uncorrelated sources, so that in Fig. 2, the OBA is preferred.

Weight functions with small separations, such as $w(1,0)$, $w(0,1)$, $w(1,1)$, and $w(1,-1)$, are also listed in Fig. 2. Notice that for the arrays mentioned herein, these weights are not small. For instance, the OBA has $w(1,0) = 15$ and $w(0,1) = 20$, due to the dense ULA on the boundaries. It is desirable to reduce $w(1,0)$, $w(0,1)$, $w(1,1)$, and $w(1,-1)$ simultaneously, so that mutual coupling can be mitigated.

III. Generalization of $\mathbb{G}_1$ in OBA

In this section, we will develop generalizations of OBA. The reason why we start with OBA is that, based on Fig. 2, they have the largest aperture for the same number of sensors, leading to the best spatial resolution.

A. *Partially Open Box Arrays (POBA)*

The main idea of partially open box arrays (POBA) is to redistribute the elements in the dense ULA, so that the weight functions for small separations decrease. In this section, we focus on the set $\mathbb{G}_1 \cup \{(0,0), (N_x - 1, 0)\}$, i.e., the N_x sensors on the bottom of Fig. 2(d). These sensors contribute to the weight function $w(1,0)$. If we can relocate some of these sensors, it is possible to reduce $w(1,0)$.

However, if we move these sensors arbitrarily, the difference coarray would no longer be hole-free and the estimation performance is degraded. Before we explain how to keep the difference coarray intact, we consider the following notations: Let $\mathbb{S}_{\text{OBA}}$ be an OBA with sizes N_x and N_y, as in Definition 3, and let $\mathbb{D}_{\text{OBA}}$, as in (6), be the difference coarray. Assume we select P distinct sensors, located at $(n_p, 0) \in \mathbb{S}_{\text{OBA}}$ for $p = 1, 2, \ldots, P$ and $P < N_x$, These sensors are relocated to P distinct locations, $(a_p, b_p) \notin \mathbb{S}_{\text{OBA}}$, yielding a new 2D array $\mathbb{S}'$ and its coarray $\mathbb{D}'$. Then we have the following lemma:

Lemma 1: $\mathbb{D}_{\text{OBA}} = \mathbb{D}'$ only if $1 \leq a_p \leq N_x - 2$ and $1 \leq b_p \leq N_y - 1$ for all $p = 1, 2, \ldots, P$, i.e., only if **the new sensor locations are inside the original array aperture**.

Proof: See Appendix A. ■

We can exculde $a_p = 0, N_x - 1$ or $b_p = 0$ in Lemma 1, since by assumption, $(a_p, b_p) \notin \mathbb{S}_{\text{OBA}}$.

Lemma 2: $\mathbb{D}_{\text{OBA}} = \mathbb{D}'$ only if $(0,0) \in \mathbb{S}'$ and $(N_x - 1, 0) \in \mathbb{S}'$, where all notations are as stated before Lemma 1.

Proof: See Appendix B. ■

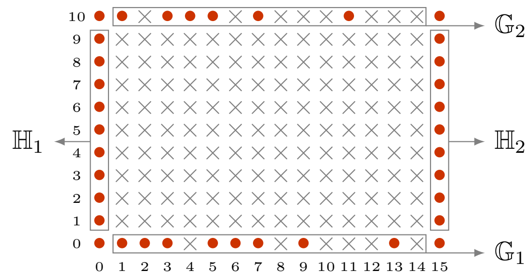

(a)

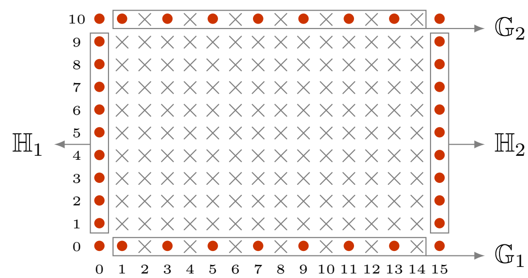

(b)

Fig. 3. Examples of POBA with $N_x = 16$ and $N_y = 11$. (a) $\mathfrak{g}_1 = \{1, 2, 3, 5, 6, 7, 9, 13\}, \mathfrak{g}_2 = \{1, 3, 4, 5, 7, 11\}$, and (b) $\mathfrak{g}_1 = \mathfrak{g}_2 = \{1, 3, 5, 7, 9, 11, 13\}$. In both cases, $\mathfrak{g}_2$ satisfies Theorem 1.

Lemma 1 and 2 indicate that for the sensors located on the bottom of OBA, only those at $(n, 0)$, where $1 \leq n \leq N_x - 2$, can be redistributed within the original aperture. For simplicity, we assume all the new sensor locations have y coordinate $N_y - 1$, i.e., $b_p = N_y - 1$ for all p in Lemma 1, which leads to the definition of POBA:

Definition 4 (Partially open box arrays, POBA): For two positive integers N_x and N_y, a partially open box array has the sensor locations defined by the integer set $\mathbb{S}_{\text{POBA}}$,

$$\mathbb{S}_{\text{POBA}} = \{(0, 0), (N_x - 1, 0), (0, N_y - 1), (N_x - 1, N_y - 1)\} \cup \mathbb{G}_1 \cup \mathbb{G}_2 \cup \mathbb{H}_1 \cup \mathbb{H}_2,$$

where $\mathbb{G}_1 = \{(n_x, 0) \mid n_x \in \mathfrak{g}_1\}$, $\mathbb{G}_2 = \{(n_x, N_y - 1) \mid n_x \in \mathfrak{g}_2\}$, $\mathbb{H}_1 = \{(0, n_y) \mid n_y \in \mathfrak{h}_1\}$, $\mathbb{H}_2 = \{(N_x - 1, n_y) \mid n_y \in \mathfrak{h}_2\}$. Here $\mathfrak{g}_1$, $\mathfrak{g}_2$, $\mathfrak{h}_1$, and $\mathfrak{h}_2$ satisfy

1) $\mathfrak{g}_1$ and $\mathfrak{g}_2$ are subsets of $\{1, 2, \ldots, N_x - 2\}$.
2) $|\mathfrak{g}_1| + |\mathfrak{g}_2| = N_x - 2$.
3) $\mathfrak{h}_1 = \mathfrak{h}_2 = \{1, 2, \ldots, N_y - 2\}$.

Note that sample MATLAB codes for POBA and all the proposed array geometries can be found in [25]. To give some feeling for POBA, let us consider two examples in Fig. 3, where $N_x = 16, N_y = 11$ and the sets $\mathbb{G}_1$, $\mathbb{G}_2$, $\mathbb{H}_1$, and $\mathbb{H}_2$ are marked in rectangles. Fig. 3(a) illustrates the POBA with $\mathfrak{g}_1 = \{1, 2, 3, 5, 6, 7, 9, 13\}$ and $\mathfrak{g}_2 = \{1, 3, 4, 5, 7, 11\}$, which are subsets of $\{1, 2, \ldots, 14\}$. Furthermore, $|\mathfrak{g}_1| + |\mathfrak{g}_2| = 8 + 6 = 14$ satisfies the second item in Definition 4. Fig. 3(b) also satisfies Definition 4. The missing elements (crosses) in $\mathbb{G}_1$ migrate to the elements (bullets) in $\mathbb{G}_2$.

Next, we will develop the difference coarray of POBA. The following theorem states a necessary and sufficient condition under which OBA and POBA share the same hole-free difference coarray:

Theorem 1: Consider an open box array and a partially open box array with the same N_x and N_y, as defined in Definition 3 and 4, respectively. Then, their difference coarrays are identical if and only if $\{\mathfrak{g}_1, N_x - 1 - \mathfrak{g}_2\}$ is a partition of $\{1, 2, \ldots, N_x - 2\}$, i.e., if and only if 1) $\mathfrak{g}_1 \cup (N_x - 1 - \mathfrak{g}_2) = \{1, 2, \ldots, N_x - 2\}$ and 2) $\mathfrak{g}_1$ and $N_x - 1 - \mathfrak{g}_2$ are disjoint. Here $N_x - 1 - \mathfrak{g}_2 = \{N_x - 1 - g \mid \forall g \in \mathfrak{g}_2\}$.

Proof: See Appendix C. ■

Let us consider some examples of Theorem 1. OBA are special cases of POBA with $\mathfrak{g}_1 = \{1, 2, \ldots, N_x - 2\}$ and $\mathfrak{g}_2$ being the empty set, which satisfy Theorem 1. For POBA in Fig. 3, the corresponding $\mathfrak{g}_1$ and $\mathfrak{g}_2$ also satisfy Theorem 1, so their difference coarrays are hole-free, and the same as $\mathbb{D}_{\text{OBA}}$.

Furthermore, Theorem 1 offers simple and straightforward design methods for POBA with hole-free difference coarrays. The first step is to choose $\mathfrak{g}_1$ to be a subset of $\{1, 2, \ldots, N_x - 2\}$. Next, $\mathfrak{g}_2$ can be uniquely determined since $\{\mathfrak{g}_1, N_x - 1 - \mathfrak{g}_2\}$ is a partition of $\{1, 2, \ldots, N_x - 2\}$. Finally, the closed-form sensor locations are given in Definition 4. The freedom in the choice of such $\mathfrak{g}_1$ can be exploited to reduce mutual coupling effects as explained next.

B. Half Open Box Arrays (HOBA)

In this subsection, we will study the *half open box array* (HOBA), which is a particular instance of POBA with reduced mutual coupling. This is done by setting $\mathfrak{g}_1$ and $\mathfrak{g}_2$ to be ULA with separation 2, so that the weight function $w(1, 0)$ is as small as 2. HOBA are defined as:

Definition 5 (Half open box arrays, HOBA): The half open box array with parameters N_x and N_y is a partially open box array with

$$\mathfrak{g}_1 = \{1 + 2\ell \mid 0 \leq \ell \leq \lfloor (N_x - 3)/2 \rfloor\}, \tag{7}$$

$$\mathfrak{g}_2 = \{N_x - 1 - 2\ell \mid 1 \leq \ell \leq \lfloor (N_x - 2)/2 \rfloor\}. \tag{8}$$

According to (7), $\mathfrak{g}_1$ represents an ULA whose left-most element is 1 and the interelement spacing is 2. It can be shown that (7) and (8) meet Theorem 1, so that the difference coarray of HOBA is the same as that of OBA, and hence, hole-free. The sensor positions for HOBA can also be obtained from Defintion 4 and 5 readily, even for large N_x and N_y.

Fig. 3(b) illustrates the HOBA with $N_x = 16$ and $N_y = 11$. It can be seen that, $|\mathfrak{g}_1| = |\mathfrak{g}_2| = 7$ and the weight functions for Fig. 3(b) are listed as follows:

$$w(1,0)=2, \;\; w(0,1)=20, \;\; w(1,1)=1, \;\; w(1,-1)=1. \tag{9}$$

Compared to the OBA in Fig. 2(d), $w(1, 0)$ decreases from 15 to 2 while $w(0, 1)$, $w(1, 1)$, and $w(1, -1)$ remain the same. To be more precise, the weight functions $w(1, 0), w(0, 1), w(1, 1), w(1, -1)$ are listed in Table I and the associated derivation can be found in Section VII-A. Therefore, the estimation performance for HOBA would be better than OBA in the presence of mutual coupling, since the weight function $w(1, 0)$ for HOBA is significantly smaller.

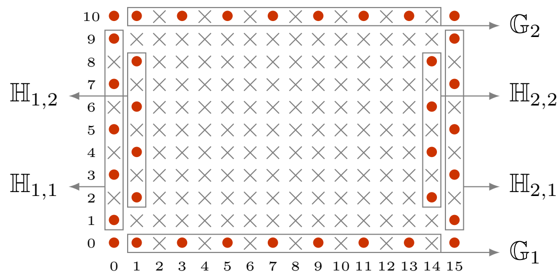

(a)

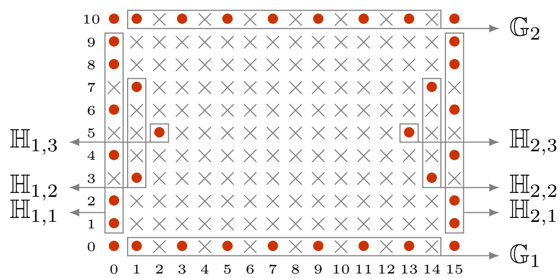

(b)

Fig. 4. Examples of POBA-L. $N_x = 16$, $N_y = 11$, $\mathfrak{g}_1 = \mathfrak{g}_2 = \{1, 3, 5, 7, 9, 11, 13\}$. (a) $\mathfrak{h}_{1,1} = \{1, 3, 5, 7, 9\}$, $\mathfrak{h}_{1,2} = \{2, 4, 6, 8\}$, $L = 2$, and (b) $\mathfrak{h}_{1,1} = \{1, 2, 4, 6, 8, 9\}$, $\mathfrak{h}_{1,2} = \{3, 7\}$, $\mathfrak{h}_{1,3} = \{5\}$, $L = 3$.

IV. Reorganization of $\mathbb{H}_1$ and $\mathbb{H}_2$ in OBA

In Section III, the set $\mathbb{G}_1$ was reorganized into $\mathbb{G}_1$ and $\mathbb{G}_2$, so that the weight function $w(1, 0)$ decreases. However, the mutual coupling effect also depends on other weight functions with small separations, such as $w(0, 1)$, $w(1, 1)$, and $w(1, -1)$. In this section, we will develop generalizations of $\mathbb{H}_1$ and $\mathbb{H}_2$ such that the new arrays are guaranteed to have hole-free coarrays. These generalizations also provide some insights to achieve smaller $w(0, 1)$, $w(1, 1)$, and $w(1, -1)$.

To begin with, let us consider HOBA, as shown in Fig. 3(b). If we redistribute the sensors in $\mathbb{H}_1$ and $\mathbb{H}_2$, it is possible to reduce the weight function $w(0, 1)$. Fig. 4 depicts some extensions of HOBA. In Fig. 4(a), $\mathbb{H}_1$ is split into two layers, $\mathbb{H}_{1,1}$ and $\mathbb{H}_{1,2}$. Such rearrangement eliminates some sensor pairs with separation $(0, 1)$ in HOBA, like the sensor pair of $(0, 2)$ and $(0, 1)$. Fig. 4(b) extends $\mathbb{H}_1$ and $\mathbb{H}_2$ into three layers, $\mathbb{H}_{1,1}$, $\mathbb{H}_{1,2}$, $\mathbb{H}_{1,3}$, and $\mathbb{H}_{2,1}$, $\mathbb{H}_{2,2}$, $\mathbb{H}_{2,3}$, respectively. In particular, the weight functions $w(0, 1)$, $w(1, 1)$, and $w(1, -1)$ are listed as follows:

Fig. 3(b):	$w(0, 1) = 20,$	$w(1, 1) = 1,$	$w(1, -1) = 1,$
Fig. 4(a):	$w(0, 1) = 4,$	$w(1, 1) = 9,$	$w(1, -1) = 9,$
Fig. 4(b):	$w(0, 1) = 8,$	$w(1, 1) = 5,$	$w(1, -1) = 5,$

It can be deduced that the arrays in Fig. 4 enjoy smaller $w(0, 1)$ than that in Fig. 3(b). Note that smaller $w(1, 0)$ and $w(0, 1)$ are typically more important in mutual coupling models [7]. Besides, it will be shown later that the arrays in Fig. 4 own hole-free coarrays.

The arrays in Fig. 4 generalize the set $\mathbb{H}_1$ and $\mathbb{H}_2$ into multiple layers $\mathbb{H}_{1,\ell}$ and $\mathbb{H}_{2,\ell}$. This concept allows us to define *partially open box arrays with L layers* (POBA-L) as follows:

Definition 6 (Partially open box arrays with L layers, POBA-L): For two positive integers N_x and N_y and a positive integer $L \leq N_x/2$, a partially open box array with L layers has the sensor locations defined by the integer set $\mathbb{S}_{\text{POBA-}L}$,

$$\mathbb{S}_{\text{POBA-}L} = \{(0,0), (N_x-1,0), (0,N_y-1), (N_x-1,N_y-1)\} \cup \mathbb{G}_1 \cup \mathbb{G}_2 \cup \left(\bigcup_{\ell=1}^{L} \mathbb{H}_{1,\ell} \cup \mathbb{H}_{2,\ell}\right),$$

where $\mathbb{G}_1 = \{(n_x,0) \mid n_x \in \mathfrak{g}_1\}$, $\mathbb{G}_2 = \{(n_x,N_y-1) \mid n_x \in \mathfrak{g}_2\}$, $\mathbb{H}_{1,\ell} = \{(\ell-1,n_y) \mid n_y \in \mathfrak{h}_{1,\ell}\}$, $\mathbb{H}_{2,\ell} = \{(N_x-\ell,n_y) \mid n_y \in \mathfrak{h}_{2,\ell}\}$. Here $\mathfrak{g}_1$, $\mathfrak{g}_2$, $\mathfrak{h}_{1,\ell}$, and $\mathfrak{h}_{2,\ell}$ satisfy

1) $\{\mathfrak{g}_1, N_x-1-\mathfrak{g}_2\}$ is a partition of $\{1,2,\ldots,N_x-2\}$.
2) $\{\mathfrak{h}_{1,\ell}\}_{\ell=1}^{L}$ is a partition of $\{1,2,\ldots,N_y-2\}$.
3) $\mathfrak{h}_{2,\ell} = N_y-1-\mathfrak{h}_{1,\ell}$ for $\ell = 1,\ldots,L$.

The first constraint on $\mathfrak{g}_1$, $\mathfrak{g}_2$ is due to Theorem 1. The second requirement indicates the sets $\mathbb{H}_{1,\ell}$ originate from $\mathbb{H}_1$ in POBA. Furthermore, the third condition enforces $\mathfrak{h}_{1,\ell}$ and $\mathfrak{h}_{2,\ell}$ to be symmetric to N_y-1, which will play a crucial role in analyzing the difference coarray. Note that, by definition, the number of sensors in POBA-L is identical to that in OBA.

Now it is clear that the arrays in Fig. 3 and Fig. 4 all satisfy Definition 6. They are characterized by different parameters L, $\mathfrak{g}_1$, and $\mathfrak{h}_{1,\ell}$. For instance, the HOBA in Fig. 3(b) corresponds to $\mathfrak{g}_1 = \{1,3,5,7,9,11,13\}$, $L=1$, and $\mathfrak{h}_{1,1} = \{1,\ldots,9\}$. The parameters for the arrays in Fig. 4 are listed in the caption.

Our next theorem determines a necessary and sufficient condition in terms of $\mathfrak{h}_{1,\ell}$ under which POBA-L have hole-free difference coarrays:

Theorem 2: Let N_x and N_y be positive integers. Let $\mathbb{D}_{\text{POBA-}L}$ be the difference coarray of a partially open box array with parameters N_x, N_y, and L layers. Let $\mathbb{D}_{\text{OBA}}$ be the difference coarray of an open box array with parameters N_x and N_y. Then $\mathbb{D}_{\text{POBA-}L} = \mathbb{D}_{\text{OBA}}$ if and only if

$$\mathfrak{h}_{1,\ell} \subseteq \mathbb{P}_{\ell'} \text{ and } \mathfrak{h}_{1,\ell} \subseteq \mathbb{P}_{\ell'} - (N_y-1), \tag{10}$$

where $\mathbb{P}_{\ell'} = \cup_{p+q=\ell'} \mathfrak{h}_{1,p} \oplus \mathfrak{h}_{1,q}$ for all $2 \leq \ell' \leq \ell$. Here $\mathbb{A} \oplus \mathbb{B} = \{a+b \mid a \in \mathbb{A}, b \in \mathbb{B}\}$ is the direct sum of $\mathbb{A}$ and $\mathbb{B}$.

Proof: See Appendix D. ■

The importance of Theorem 2 resides in the following: Since the sets $\mathfrak{h}_{1,\ell}$ have smaller sizes than the 2D array $\mathbb{S}_{\text{POBA-}L}$, it is more tractable to verify (10) than to calculate $\mathbb{D}_{\text{POBA-}L}$ directly. Furthermore, if (10) is *not* satisfied, then all the holes in $\mathbb{D}_{\text{POBA-}L}$ can be identified from the 1D sets $\mathfrak{h}_{1,\ell}$, based on the necessity proof of Theorem 2. This is also demonstrated through a numerical example in [31, Section I]. Another advantage is that, we can use (10) to design new array configurations with reduced mutual coupling. By choosing $\mathfrak{h}_{1,\ell}$ appropriately, it is possible to reduce the weight function $w(0,1)$, $w(1,1)$, and $w(1,-1)$ systematically.

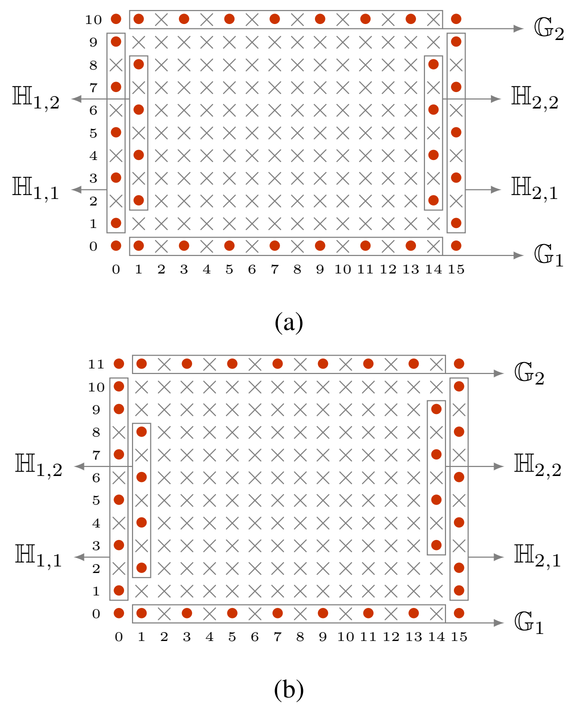

Fig. 5. Examples of HOBA-2. (a) $N_x = 16, N_y = 11$ and (b) $N_x = 16, N_y = 12$.

In Section V and VI, we will propose half open box arrays with two layers and hourglass arrays, respectively. These arrays not only have simple, closed-form sensor locations but also satisfy Theorem 2, so that their difference coarrays are hole-free. The weight functions of these novel array configurations will be summarized in Section VII.

V. Half Open Box Arrays with Two Layers (HOBA-2)

We now introduce *the half open box array with two layers* (HOBA-2). This array is defined by choosing $\mathfrak{h}_{1,2}$ to be ULA with separation 2, so that the weight function $w(0,1)$ decreases. The formal definition is given as follows:

Definition 7 (Half open box arrays with two layers, HOBA-2): The half open box array with two layers is a partially open box array with $L = 2$ layers, and

$$\mathfrak{g}_1 = \{1 + 2\ell \mid 0 \leq \ell \leq \lfloor (N_x - 3)/2 \rfloor\},$$

$$\mathfrak{g}_2 = \{N_x - 1 - 2\ell \mid 1 \leq \ell \leq \lfloor (N_x - 2)/2 \rfloor\},$$

$$\mathfrak{h}_{1,1} = \{1 + 2\ell \mid 0 \leq \ell \leq \lfloor (N_y - 3)/2 \rfloor\} \cup \{N_y - 2\},$$

$$\mathfrak{h}_{1,2} = \{2\ell \mid 1 \leq \ell \leq \lfloor (N_y - 3)/2 \rfloor\}.$$

The sets $\mathfrak{h}_{2,1}$ and $\mathfrak{h}_{2,2}$ satisfy Definition 6.

Fig. 5 depicts the array geometry of HOBA-2 for (a) $N_y = 11$ (odd) and (b) $N_y = 12$ (even). It can be observed that the weight function $w(0,1)$ becomes smaller than HOBA with the same N_x and N_y. For instance, for HOBA with $N_x = 16$ and $N_y = 11$, $w(0,1)$ is 20 while the weight function $w(0,1)$ for HOBA-2, $N_x = 16$, and $N_y = 11$, as shown in Fig. 5(a), is as small as 4.

The difference coarray for HOBA-2 possess the same difference coarray as OBA, as indicated in the following theorem:

Theorem 3: Half open box arrays with two layers have the same difference coarray as open box arrays.

Proof: According to Theorem 2, it suffices to show that

$$\mathfrak{h}_{1,2} \subseteq \mathbb{P}_2 = \mathfrak{h}_{1,1} \oplus \mathfrak{h}_{1,1}, \tag{11}$$

$$\mathfrak{h}_{1,2} \subseteq \mathbb{P}_2 - (N_y - 1) = \mathfrak{h}_{1,1} \oplus \mathfrak{h}_{1,1} - (N_y - 1). \tag{12}$$

Eq. (11) can be proved as follows. Since $1 \in \mathfrak{h}_{1,1}$, we have

$$\mathfrak{h}_{1,1} \oplus \mathfrak{h}_{1,1} \supseteq \mathfrak{h}_{1,1} + 1 \supseteq \{2 + 2\ell \mid 0 \leq \ell \leq \lfloor (N_x - 3)/2 \rfloor\}.$$

Letting $\ell' = \ell + 1$ yields

$$\mathfrak{h}_{1,1} \oplus \mathfrak{h}_{1,1} \supseteq \{2\ell' \mid 1 \leq \ell' \leq \lfloor (N_x - 3)/2 \rfloor + 1\} \supset \mathfrak{h}_{1,2}.$$

Next we will prove (12). It can be observed that $N_y - 2 \in \mathfrak{h}_{1,1}$ whenever N_y is odd or even. Then we have

$$\mathfrak{h}_{1,1} \oplus \mathfrak{h}_{1,1} - (N_y - 1) \supseteq \mathfrak{h}_{1,1} \oplus \{N_y - 2\} - (N_y - 1)$$

$$\supseteq \{2\ell \mid 0 \leq \ell \leq \lfloor (N_y - 3)/2 \rfloor\} \supset \mathfrak{h}_{1,2}.$$

This completes the proof. ■

The mutual coupling effect depends not only on $w(0, 1)$, but also on other weight functions at small separations, such as $w(1, 1)$ and $w(1, -1)$. For HOBA-2, even though the weight function $w(0, 1)$ becomes smaller, $w(1, 1)$ and $w(1, -1)$ increase significantly. For instance, the HOBA with $N_x = 16, N_y = 11$, as depicted in Fig. 3(b), enjoys $w(1, 1) = w(1, -1) = 1$ while the HOBA-2 and $N_x = 16, N_y = 11$, as illustrated in Fig. 5(a), owns $w(1, 1) = w(1, -1) = 9$. Therefore, for HOBA-2, the reduction in the mutual coupling effect is limited.

VI. Hourglass Arrays

In this section, we will propose *hourglass arrays*, which look like hourglasses on the 2D plane. These novel array configurations have the same number of sensors and the same difference coarray as those in OBA. Therefore, the difference coarrays of hourglass arrays are hole-free. In addition, the sensor locations can be expressed in closed form. Most importantly, they possess small weight functions $w(1, 0)$ and $w(0, 1)$ as well as $w(1, 1)$ and $w(1, -1)$.

To develop some feeling for hourglass arrays, Fig. 4(b) demonstrates the hourglass array with $N_x = 16$ and $N_y = 11$. The sets $\mathfrak{g}_1$ and $\mathfrak{g}_2$ are identical to those in HOBA. There are $L = 3$ layers. The sensors in $\mathbb{H}_{1,1} \cup \mathbb{H}_{1,2} \cup \mathbb{H}_{1,3}$ can be viewed as the unions of three ULAs. The first ULA contains $(0, 2), (0, 4), (0, 6), (0, 8)$, the second ULA is composed of $(0, 1), (1, 3), (2, 5)$, and the third ULA consists of $(0, 9), (1, 7), (2, 5)$. Notice that the sensor located at $(2, 5)$ is relatively far away from other sensors, since the distance from $(2, 5)$ to its nearest sensor is $\sqrt{5}$.

The hourglass arrays are formally defined as

$$\mathfrak{h}_{1,\ell} = \begin{cases} \{2p,\ N_y-1-2p \mid 1 \le p \le \lfloor (N_y-1)/4 \rfloor\} \cup \{1,\ N_y-2\}\,, & \text{if } \ell = 1, \\ \{2\ell-1,\ N_y-2\ell\}\,, & \text{if } N_y \text{ is odd and } 2 \le \ell \le L, \\ \{2\ell-1,\ 2\lfloor N_y/4 \rfloor - 2\ell+3,\ 2\lceil N_y/4 \rceil + 2\ell - 4,\ N_y-2\ell\}, & \text{if } N_y \text{ is even and } 2 \le \ell \le L, \end{cases} \tag{13}$$

Definition 8 (Hourglass arrays): Let N_x and N_y be positive integers. An hourglass array is a partially open box array with L layers where the sets $\mathfrak{g}_1$ and $\mathfrak{g}_2$ are given by

$$\mathfrak{g}_1 = \{1 + 2p \mid 0 \le p \le \lfloor (N_x-3)/2 \rfloor\},$$

$$\mathfrak{g}_2 = \{N_x - 1 - 2p \mid 1 \le p \le \lfloor (N_x-2)/2 \rfloor\}.$$

Here the number of layers L is defined as

$$L = \begin{cases} \lfloor (N_y+1)/4 \rfloor\,, & \text{if } N_y \text{ is odd}, \\ \lfloor N_y/8 + 1 \rfloor\,, & \text{if } N_y \text{ is even}. \end{cases} \tag{14}$$

The sets $\mathfrak{h}_{1,\ell}$ are given in (13) and $\mathfrak{h}_{2,\ell} = N_y - 1 - \mathfrak{h}_{1,\ell}$.

The MATLAB function `POBA_L.m` returns the sensor locations of hourglass arrays, by specifying the parameter N_x, N_y, and the third parameter being `'hourglass'` [25]. Fig. 6 elaborates the array geometry of hourglass arrays for (a) $N_x = 15$, $N_y = 27$ and (b) $N_x = 15$, $N_y = 26$. It can be seen from Fig. 6(a) that, when N_y is an odd number, The array configuration, indicated by the bullets as the sensors, resembles an hourglass. The sets $\mathbb{G}_1, \mathbb{G}_2, \mathbb{H}_{1,\ell}, \mathbb{H}_{2,\ell}$ for $2 \le \ell \le L = 7$, constitute the two bulbs in an hourglass. The neck in this hourglass corresponds to $\mathbb{H}_{1,7}$ and $\mathbb{H}_{2,7}$. The sets $\mathbb{H}_{1,1}$ and $\mathbb{H}_{2,1}$ can be regarded as two pillars. If N_y is an even number, as shown in Fig. 6(b), the array geometry looks like an hourglass ($\mathbb{G}_1, \mathbb{G}_2, \mathbb{H}_{1,\ell}, \mathbb{H}_{2,\ell}$ for $2 \le \ell \le L = 4$) with two necks ($\mathbb{H}_{1,4}, \mathbb{H}_{2,4}$) and two pillars ($\mathbb{H}_{1,1}, \mathbb{H}_{2,1}$).

Note that the number of layers L depends on N_y. According to (14), L is approximately $N_y/4$ if N_y is odd while L is around $N_y/8$ when N_y is even. Furthermore, $L \le N_x/2$ in the defintion of POBA-L (Defintion 6). It can be deduced that, for large N_x and N_y, the aspect ratio N_y/N_x of hourglass arrays should be less than 2 for odd N_y and 4 for even N_y.

The next result characterizes the difference coarray of hourglass arrays:

Theorem 4: Hourglass arrays own the same difference coarray as open box arrays.

Proof: See Appendix E. ■

Summarizing, hourglass arrays own closed-form sensor locations and their coarrays are identical to those of OBA. Furthermore, it will be shown in the next section that, the weight functions $w(1,0)$, $w(0,1)$, $w(1,1)$, and $w(1,-1)$ for hourglass arrays are sufficiently small, so that the mutual coupling effect can be significantly reduced.

VII. Weight functions

It is known that the weight functions at small separations are more important for mutual coupling effects [7]. It is desirable to have sufficiently small $w(1,0)$, $w(0,1)$, $w(1,1)$, and $w(1,-1)$. Therefore, in this section, we will

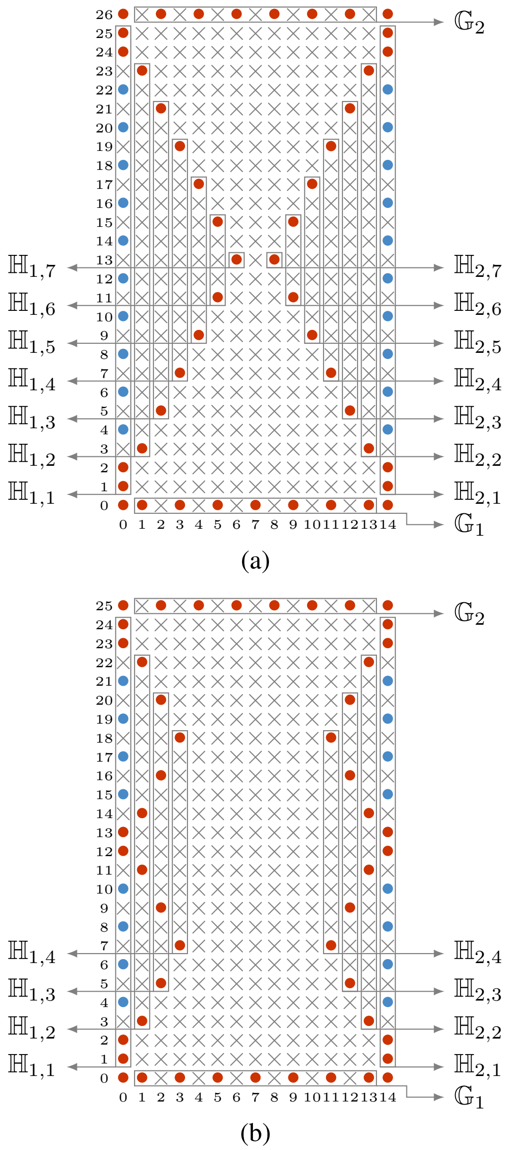

Fig. 6. Hourglass arrays with (a) $N_x = 15, N_y = 27$ and (b) $N_x = 15, N_y = 26$. The total number of sensors for (a) and (b) are 67 and 65, respectively.

study these weight functions for URA, billboard arrays, OBA, HOBA, HOBA-2, and hourglass arrays. A summary is given in Table I for convenience. Note that some assumptions on the first row of Table I (e.g., $N_x \geq 3$ and $N_y \geq 2$ for the OBA) are not parts of the definitions for these arrays. They are introduced in order to have simple and closed-form expressions for the weight functions.

Consider the weight function $w(1, 0)$ for all these arrays. Asymptotically, $w(1, 0)$ grows linearly with N_xN_y for URA. For billboard arrays and OBA, $w(1, 0)$ increases linearly with N_x. It is noteworthy that, for the proposed array configurations (HOBA, HOBA-2, and hourglass arrays), the weight function $w(1, 0)$ is fixed to be 2, even if N_x and N_y are huge.

However, mutual coupling effects also depend on $w(0, 1)$, $w(1, 1)$, and $w(1, -1)$. According to Table I, hourglass

TABLE I

SUMMARY ON THE WEIGHT FUNCTIONS

	URA	Billboard	OBA	HOBA	HOBA-2	Hourglass arrays
		$N_x = N_y \geq 4$	$N_x \geq 3$, $N_y \geq 2$	$N_x \geq 4$, $N_y \geq 3$	$N_x \geq 5$, $N_y \geq 5$	$N_x \geq 2L+1$, $N_y \geq 7$, L is defined in (14).
$w(1,0)$	$N_y(N_x-1)$	N_x-1	N_x-1	2	2	2
$w(0,1)$	$N_x(N_y-1)$	N_y-1	$2(N_y-1)$	$2(N_y-1)$	$\begin{cases} 4, & \text{if } N_y \text{ is odd,} \\ 6, & \text{if } N_y \text{ is even.} \end{cases}$	$\begin{cases} 8, & \text{if } N_y \text{ is odd,} \\ 10, & \text{if } N_y \text{ is even.} \end{cases}$
$w(1,1)$	$(N_x-1)(N_y-1)$	N_x-3	1	1	$\begin{cases} N_y-2, & \text{if } N_y \text{ is odd,} \\ N_y-3, & \text{if } N_y \text{ is even.} \end{cases}$	$\begin{cases} 3, & \text{if } N_y = 7, 8, \\ 5, & \text{if } N_y = 10 \text{ or } 2r+1,\ r \geq 4, \\ 7, & \text{if } N_y = 4r,\ r \geq 3, \\ 9, & \text{if } N_y = 4r+2,\ r \geq 3. \end{cases}$
$w(1,-1)$	$(N_x-1)(N_y-1)$	1	1	1	$\begin{cases} N_y-2, & \text{if } N_y \text{ is odd,} \\ N_y-3, & \text{if } N_y \text{ is even.} \end{cases}$	$\begin{cases} 3, & \text{if } N_y = 7, 8, \\ 5, & \text{if } N_y = 10 \text{ or } 2r+1,\ r \geq 4, \\ 7, & \text{if } N_y = 4r,\ r \geq 3, \\ 9, & \text{if } N_y = 4r+2,\ r \geq 3. \end{cases}$

arrays are the only class of arrays for which all the weight functions, such as $w(1,0)$, $w(0,1)$, $w(1,1)$, and $w(1,-1)$ are significantly smaller when N_x and N_y are large. This property indicates that hourglass arrays own the least mutual coupling among all the arrays listed in Table I.

Next, we will justify the expressions for some of the weight functions given in Table I.

A. Derivation to the weight function expressions in HOBA

To evaluate $w(1,0)$, it suffices to consider the elements whose y coordinates are either 0 or N_y-1, due to Definition 4. Since $N_x \geq 4$, $\mathfrak{g}_1$ and $\mathfrak{g}_2$ are not empty. It is obvious that the sensor pair of $(1,0)$ and $(0,0)$ contributes to $w(1,0)$. First consider N_x to be an odd number. According to (7), $N_x-2 \in \mathfrak{g}_1$, so $(N_x-1,0)$ and $(N_x-2,0)$ also contribute to $w(1,0)$. In this case, the smallest and the largest elements in $\mathfrak{g}_2$ are 2 and N_x-3, respectively, implying there are no sensor pairs with separation 1 if the y coordinates are N_y-1. On the other hand, if N_x is even, the only two sensor pairs contributing to $w(1,0)$ are $(1,0),(0,0)$ and $(1,N_y-1),(0,N_y-1)$.

The weight function $w(0,1)$ is identical to that in OBA since they share the same $\mathbb{H}_1$ and $\mathbb{H}_2$. The weight functions $w(1,1)$ and $w(1,-1)$ can be calculated as follows: If N_x is odd, the sensor pairs $(N_x-1,1),(N_x-2,0)$ and $(1,0),(0,1)$ contribute to $w(1,1)$ and $w(1,-1)$, respectively. If N_x is even, $w(1,1)$ and $w(1,-1)$ result from the sensor pairs $(1,N_y-1),(0,N_y-2)$ and $(1,0),(0,1)$, which completes the derivation.

B. Derivation to the weight function expressions in HOBA-2

The weight function $w(1,0)$ is 2 because the sets $\mathfrak{g}_1$ and $\mathfrak{g}_2$ in HOBA-2. are exactly the same as those in HOBA.

Next we will derive the expression for $w(0,1)$. If N_y is an odd number, it can be deduced that $1 \in \mathfrak{h}_{1,1}$, $N_y-2 \in \mathfrak{h}_{1,1}$, and $N_y-3 \notin \mathfrak{h}_{1,1}$. Hence, the four sensor pairs contributing to $w(0,1)$ are $(0,1),(0,0)$; $(0,N_y-1),(0,N_y-2)$;

$(N_x-1,1),(N_x-1,0)$; $(N_x-1,N_y-1),(N_x-1,N_y-2)$. If N_y is an even number, we have $1 \in \mathfrak{h}_{1,1}$, $N_y-2 \in \mathfrak{h}_{1,1}$, and $N_y-3 \in \mathfrak{h}_{1,1}$. Apart from the four sensor pairs in the odd case, the two more pairs are $(0,N_y-2),(0,N_y-3)$ and $(N_x-1,2),(N_x-1,1)$. The remaining sensor pairs do not add to $w(0,1)$ since the separations are greater than 1.

The weight function $w(1,1)$ can be obtained as follows: For $w(1,1)$, it suffices to consider the cross differences between $\mathbb{H}_{1,1}$ and $\mathbb{H}_{1,2}$, as well as $\mathbb{H}_{2,1}$ and $\mathbb{H}_{2,2}$. It can be inferred that the sensor pairs of $(1,2\ell) \in \mathbb{H}_{1,2}$ and $(0,2(\ell-1)+1) \in \mathbb{H}_{1,1}$ contribute to $w(1,1)$. In this case, there are $|\mathfrak{h}_{1,2}|$ pairs. Similar arguments also apply to the sets $\mathbb{H}_{2,1}$ and $\mathbb{H}_{2,2}$. Next, if N_x is odd, the sensor pair $(N_x-1,1),(N_x-2,0)$ also has separation $(1,1)$. On the other hand, if N_x is even, the sensor pair $(1,N_y-1),(0,N_y-2)$ contributes to $w(1,1)$. Therefore, $w(1,1)$ becomes is

$$\begin{aligned} w(1,1) &= 2|\mathfrak{h}_{1,2}|+1 = 2\lfloor (N_y-3)/2 \rfloor + 1 \\ &= \begin{cases} N_y-2, & \text{if } N_y \text{ is odd,} \\ N_y-3, & \text{if } N_y \text{ is even.} \end{cases} \end{aligned}$$

The same technique can be used in finding the expression for $w(1,-1)$.

C. Derivation to the weight function expressions in hourglass arrays

It can be deduced that the weight function $w(1,0)$ is also 2, since the sets $\mathfrak{g}_1$ and $\mathfrak{g}_2$ share the same expression as those in HOBA.

To derive expressions for $w(0,1)$, consider the following chain of arguments. Since $N_y \geq 7$, we have $\lfloor (N_y-1)/4 \rfloor \geq 1$, so $2 \in \mathfrak{h}_{1,1}$ and $N_y-3 \in \mathfrak{h}_{1,1}$. As a result, there exist eight sensor pairs

$$(n_x, n_y+1), \ (n_x, n_y) \tag{15}$$

where $n_x = 0,\ N_x-1$, and $n_y = 0,\ 1,\ N_y-3,\ N_y-2$, contributing to the weight function $w(0,1)$.

For other sensor pairs, the self difference of $\mathfrak{h}_{1,1}$ is first analyzed. Consider the following two sets,

$$\begin{aligned} \mathfrak{h}_{1,1}^{+} &= \{N_y-1-2p \mid 1 \leq p \leq \lfloor (N_y-1)/4 \rfloor\}, \\ \mathfrak{h}_{1,1}^{-} &= \{2p \mid 1 \leq p \leq \lfloor (N_y-1)/4 \rfloor\}, \end{aligned}$$

which satisfy $\mathfrak{h}_{1,1} = \mathfrak{h}_{1,1}^{+} \cup \mathfrak{h}_{1,1}^{-} \cup \{1, N_y-2\}$. The self difference of $\mathfrak{h}_{1,1}$ can be decomposed into the self differences and the cross differences of $\mathfrak{h}_{1,1}^{+}$, $\mathfrak{h}_{1,1}^{-}$, and $\{1, N_y-2\}$. Since $\mathfrak{h}_{1,1}^{+}$ and $\mathfrak{h}_{1,1}^{-}$ are ULA with spacing 2, for $w(0,1)$, it suffices to consider the cross differences between $\mathfrak{h}_{1,1}^{+}$ and $\mathfrak{h}_{1,1}^{-}$, defined as

$$\mathrm{diff}(\mathfrak{h}_{1,1}^{+}, \mathfrak{h}_{1,1}^{-}) = \{a-b \mid \forall\, a \in \mathfrak{h}_{1,1}^{+},\ \forall\, b \in \mathfrak{h}_{1,1}^{-}\}.$$

The minimum element in $\mathrm{diff}(\mathfrak{h}^+_{1,1}, \mathfrak{h}^-_{1,1})$ is given by

$$N_y - 1 - 4\lfloor (N_y-1)/4 \rfloor = \begin{cases} 0, & \text{if } N_y = 4r+1, \\ 1, & \text{if } N_y = 4r+2, \\ 2, & \text{if } N_y = 4r+3, \\ 3, & \text{if } N_y = 4r, \end{cases} \tag{16}$$

Therefore, if $N_y = 4r+2$, we have $1 \in \mathrm{diff}(\mathfrak{h}_{1,1}, \mathfrak{h}_{1,1})$. Similarly, it can be shown that $1 \in \mathrm{diff}(\mathfrak{h}_{2,1}, \mathfrak{h}_{2,1})$, since $\mathfrak{h}_{2,1} = N_y - 1 - \mathfrak{h}_{1,1}$.

Next we turn to the self differences of $\mathfrak{h}_{1,\ell}$ for $2 \leq \ell \leq L$. If N_y is odd, we will show that the difference $(0,1)$ cannot be found in the self difference of $\mathfrak{h}_{1,\ell}$. This statement can be proved as follows. According to (13), the self difference of $\mathfrak{h}_{1,\ell}$ is

$$\mathrm{diff}(\mathfrak{h}_{1,\ell}, \mathfrak{h}_{1,\ell}) = \{0, \pm(N_y + 1 - 4\ell)\}.$$

Since N_y is odd, all the elements in $\mathrm{diff}(\mathfrak{h}_{1,\ell}, \mathfrak{h}_{1,\ell})$ are even numbers, so $1 \notin \mathrm{diff}(\mathfrak{h}_{1,\ell}, \mathfrak{h}_{1,\ell})$.

If N_y is even, the self difference of $\mathfrak{h}_{1,\ell}$ becomes

$$\begin{aligned} \mathrm{diff}(\mathfrak{h}_{1,\ell}, \mathfrak{h}_{1,\ell}) = \{0, &\pm(s_2 - s_1), \pm(s_3 - s_1), \pm(s_4 - s_1), \\ &\pm(s_3 - s_2), \pm(s_4 - s_2), \pm(s_4 - s_3)\}, \end{aligned}$$

where $s_1 = 2\ell - 1$, $s_2 = 2\lfloor N_y/4 \rfloor - 2\ell + 3$, $s_3 = 2\lceil N_y/4 \rceil + 2\ell - 4$, and $s_4 = N_y - 2\ell$, as indicated in (13). It can be shown that $s_1 < s_2 < s_3 < s_4$. Therefore, for $w(0,1)$, it suffices to consider the differences between adjacent elements, as discussed in the following three cases:

1) $s_2 - s_1 = 2\lfloor N_y/4 \rfloor - 4\ell + 4$ is an even number, which cannot be 1.
2) $s_3 - s_2 = 2(\lceil N_y/4 \rceil - \lfloor N_y/4 \rfloor) + (4\ell - 7)$ is an odd number. If $s_3 - s_2 = 1$, then we have

$$\lceil N_y/4 \rceil - \lfloor N_y/4 \rfloor = 4 - 2\ell. \tag{17}$$

   Since $\lceil x \rceil - \lfloor x \rfloor$ is 0 if x is an integer and 1 otherwise, the solution to (17) is $\ell = 2$ and $N_y = 4r$ for some integer r. That is, if N_y is an integer multiple of 4, there exists a sensor pair in $\mathfrak{h}_{1,2}$ with separation 1.
3) $s_4 - s_3 = N_y - 2\lceil N_y/4 \rceil - 4\ell + 4$ is an even number.

Similar arguments can be applied to $\mathfrak{h}_{2,\ell}$. The expressions for $w(0,1)$ in hourglass arrays can be obtained by combining (15), (16), and (17).

For $w(1,1)$, we first consider the sensor pairs $\mathbf{n}_1, \mathbf{n}_2$ such that $\mathbf{n}_1 - \mathbf{n}_2 = (1,1)$ for $N_y = 7, 8, 10$ and odd N_x, as listed in the first three rows of Table II. Next we will focus on the remaining cases in Table II.

1) $N_y = 2r + 1$ and N_x is an odd number, where $r \geq 4$ is an integer: In this case, $L \geq 2$ and $\lfloor (N_y-1)/4 \rfloor \geq 2$. Therefore, we have

$$\{2,\ 4,\ N_y - 5,\ N_y - 3\} \subseteq \mathfrak{h}_{1,1}, \tag{18}$$

$$\{3,\ N_y - 4\} \subseteq \mathfrak{h}_{1,2}. \tag{19}$$

TABLE II

SENSOR PAIRS FOR $w(1,1)$ WITH ODD N_x

	Sensor pairs $\mathbf{n}_1, \mathbf{n}_2$;
$N_y = 7$	$(1,3),(0,2)$; $(N_x-1,1),(N_x-2,0)$; $(N_x-1,4),(N_x-2,3)$;
$N_y = 8$	$(1,3),(0,2)$; $(N_x-1,1),(N_x-2,0)$; $(N_x-1,5),(N_x-2,4)$;
$N_y = 10$	$(1,3),(0,2)$; $(1,6),(0,5)$; $(N_x-1,1),(N_x-2,0)$; $(N_x-1,4),(N_x-2,3)$; $(N_x-1,7),(N_x-2,6)$;
$N_y = 2r+1$, $r \geq 4$	$(1,3),(0,2)$; $(1,N_y-4),(0,N_y-5)$; $(N_x-1,1),(N_x-2,0)$; $(N_x-1,4),(N_x-2,3)$; $(N_x-1,N_y-3),(N_x-2,N_y-4)$;
$N_y = 4r$, $r \geq 3$	$(1,3),(0,2)$; $(1,2r-1),(0,2r-2)$; $(1,N_y-4),(0,N_y-5)$; $(N_x-1,1),(N_x-2,0)$; $(N_x-1,4),(N_x-2,3)$; $(N_x-1,2r+1),(N_x-2,2r)$; $(N_x-1,N_y-3),(N_x-2,N_y-4)$;
$N_y = 4r+2$, $r \geq 3$	$(1,3),(0,2)$; $(1,2r-1),(0,2r-2)$; $(1,2r+2),(0,2r+1)$; $(1,N_y-4),(0,N_y-5)$; $(N_x-1,1),(N_x-2,0)$; $(N_x-1,4),(N_x-2,3)$; $(N_x-1,2r),(N_x-2,2r-1)$; $(N_x-1,2r+3),(N_x-2,2r+2)$; $(N_x-1,N_y-3),(N_x-2,N_y-4)$;

Due to (18) and (19), the only five sensor pairs are listed in the fourth row of Table II. It can be shown that there do not exist sensor pairs with separation $(1,1)$ within $\mathbb{H}_{1,\ell}$ and $\mathbb{H}_{2,\ell}$ for $2 \leq \ell \leq L$.

2) $N_y = 4r$ and N_x is an odd number, where $r \geq 3$ is an integer: In this case, we know that

$$L = \lfloor 4r/8 + 1 \rfloor \geq \lfloor 12/8 + 1 \rfloor = 2, \tag{20}$$

$$\lfloor (N_y - 1)/4 \rfloor = \lfloor (4r-1)/4 \rfloor = r - 1 \geq 2. \tag{21}$$

Using (20) and (21) in (13) leads to

$$\{2,\ 4,\ 2r-2,\ 2r+1,\ N_y-5,\ N_y-3\} \subseteq \mathfrak{h}_{1,1}, \tag{22}$$

$$\{3,\ 2r-1,\ 2r,\ N_y-4\} \subseteq \mathfrak{h}_{1,2}. \tag{23}$$

As a result, the seven sensor pairs contributing to the difference $(1,1)$ are shown in the fifth row of Table II.

3) $N_y = 4r+2$ and N_x is an odd number, where $r \geq 3$ is an integer. Similar to (20) and (21), we have $L \geq 2$ and $\lfloor (N_y-1)/4 \rfloor = r \geq 3$, implying

$$\{2,\ 4,\ 2r-2,\ 2r,\ 2r+1,\ 2r+3,\ N_y-5,\ N_y-3\} \subseteq \mathfrak{h}_{1,1}, \tag{24}$$

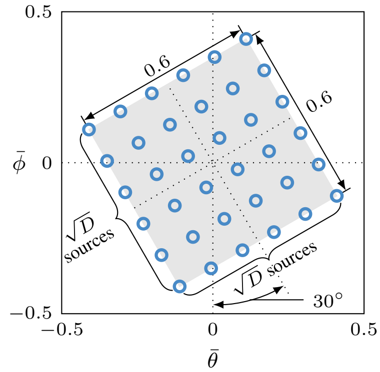

Fig. 7. The normalized source directions, as shown in circles, for the examples in Section VIII. Here the number of sources D is assumed to be a perfect square, i.e., $\sqrt{D}$ is an integer. The sources are uniformly located in the shaded region, over which there are $\sqrt{D}$ equally-spaced sources in one way and $\sqrt{D}$ equally-spaced sources in the other.

$$\{3,\ 2r-1,\ 2r+2,\ N_y-4\} \subseteq \mathfrak{h}_{1,2}. \tag{25}$$

Based on (24) and (25), the nine sensor pairs can be found to be those in the last row of Table II.

If N_x is an even number, it can be shown that $N_x - 2 \notin \mathfrak{g}_1$ and $1 \in \mathfrak{g}_2$. Therefore the sensor pair $(N_x - 1, 1), (N_x - 2, 0)$ does not exist. Instead, another sensor pair $(1, N_y - 1), (0, N_y - 2)$ contributes to $w(1, 1)$ for even N_x. The remaining sensor pairs are listed in Table II.

For the weight function $w(1, -1)$, the associated sensor pairs can also be identified using Table II. Let $\mathbf{n}_1$ and $\mathbf{n}_2$ be a sensor pair satisfying $\mathbf{n}_1 - \mathbf{n}_2 = (1, 1)$. Based on $\mathbf{n}_1$ and $\mathbf{n}_2$, we can uniquely construct another sensor pair $\mathbf{n}_1'$ and $\mathbf{n}_2'$ such that $\mathbf{n}_1' - \mathbf{n}_2' = (1, -1)$, as follows:

1) If $\mathbf{n}_1 = (n_{1x}, n_{1y}) \in \mathbb{H}_{1,1}$ and $\mathbf{n}_2 = (n_{2x}, n_{2y}) \in \mathbb{H}_{1,2}$ such that $\mathbf{n}_1 - \mathbf{n}_2 = (1, 1)$, then it can be shown that the sensor pair

$$\mathbf{n}_1' = (n_{1x}, N_y - 1 - n_{1y}), \qquad \mathbf{n}_2' = (n_{2x}, N_y - 1 - n_{2y}),$$

satisfies $\mathbf{n}_1' \in \mathbb{H}_{1,1}$, $\mathbf{n}_2' \in \mathbb{H}_{1,2}$, and $\mathbf{n}_1' - \mathbf{n}_2' = (1, -1)$. This property holds true since $\mathfrak{h}_{1,\ell}$ is symmetric. Similar arguments apply to $\mathbf{n}_1 = (n_{1x}, n_{1y}) \in \mathbb{H}_{2,1}$ and $\mathbf{n}_2 = (n_{2x}, n_{2y}) \in \mathbb{H}_{2,2}$.

2) For odd N_x, if $\mathbf{n}_1 = (N_x - 1, 1)$ and $\mathbf{n}_2 = (N_x - 2, 0)$, it can be proved that $\mathbf{n}_1' = (1, 0) \in \mathbb{G}_1$, $\mathbf{n}_2' = (0, 1) \in \mathbb{H}_{1,1}$, and $\mathbf{n}_1' - \mathbf{n}_2' = (1, -1)$.

3) For even N_x, if $\mathbf{n}_1 = (1, N_y - 1)$ and $\mathbf{n}_2 = (0, N_y - 2)$, then the sensor pair becomes $\mathbf{n}_1' = (1, 0)$ and $\mathbf{n}_2' = (0, 1)$.

Therefore, we have $w(1, -1) = w(1, 1)$ in hourglass arrays.

VIII. Numerical Examples

In this section, we will study the DOA estimation performance in the presence of mutual coupling, for URA, billboard arrays, 2D nested arrays, OBA, HOBA, HOBA-2, and hourglass arrays. The parameters are chosen to be $N_x = N_y = 9$ for URA, $N_x = N_y = 28$ for billboard arrays, $N_1 = 4, N_2 = 5$ for 2D nested arrays,

$N_x = 29, N_y = 27$ for OBA, HOBA, HOBA-2, and hourglass arrays, where the notations are given in Fig. 2 to 6. The array geometries are also illustrated in [31, Section II] for clarity. Therefore, the number of physical sensors is fixed to be 81 for all these arrays. The aperture is 8×8 for URA, 27×27 for billboard arrays, 24×24 for 2D nested arrays, and 26×28 for OBA, HOBA, HOBA-2, as well as hourglass arrays. There are D, uncorrelated, equal-power sources with 0dB SNR. The number of snapshots K is 200, and the normalized DOAs are illustrated in Fig. 7, where the number of sources D is assumed to be a square number. The mutual coupling model is given in (5), where $c(1) = 0.3$, $B = 5$, and $c(\ell) = c(1)e^{j\pi(\ell-1)/4}/\ell$. The measurements are generated based on (4) and the DOAs are estimated using the 2D unitary ESPRIT algorithm [32] on the finite snapshot version of the signal on the difference coarray. The root-mean-squared error is defined as $\mathrm{RMSE} = ((1/D)\sum_{i=1}^{D}(\widehat{\bar{\theta}}_i - \bar{\theta}_i)^2 + (\widehat{\bar{\phi}}_i - \bar{\phi}_i)^2)^{1/2}$, where $(\bar{\theta}_i, \bar{\phi}_i)$ and $(\widehat{\bar{\theta}}_i, \widehat{\bar{\phi}}_i)$ are the true normalized DOA and the estimated normalized DOA of the ith source, respectively. Note that mutual coupling is present in the measurements but the 2D unitary ESPRIT algorithm does not take care of mutual coupling. This scenario offers a baseline performance for DOA estimation in the presence of mutual coupling. It will be shown that the proposed 2D sparse arrays (HOBA, HOBA-2, and hourglass arrays) are capable of estimating the DOA satisfactorily when mutual coupling is present, even if the DOA estimator does not take into account the existence of this coupling.

Fig. 8(a) shows the estimation performance as a function of SNR. Here the number of sources $D = 9$. At 0dB SNR, the least RMSE is exhibited by hourglass arrays, followed by HOBA-2, then HOBA, then billboard arrays, then OBA, then 2D nested arrays, and finally URA. Note that this result is in accordance with the associated weight functions, as listed in Table I. Qualitatively, the smaller the weight functions $w(1,0), w(0,1), w(1,1), w(1,-1)$ are, the less the mutual coupling effects are. The dependence of the RMSE versus the number of snapshots K is plotted in Fig. 8(b). It is noteworthy that, in the presence of mutual coupling, hourglass arrays demonstrate considerable reduction on RMSE using only 40 snapshots.

Fig. 9 shows the dependence of the RMSE on the parameter c_1 in the mutual coupling model. It can be observed that, for any array configuration, the RMSE is small if c_1 is close to 0 (less mutual coupling), and the error starts to increase significantly above certain thresholds of c_1. In Fig. 9(a), the number of sources is $D = 9$. It can be deduced that the thresholds of c_1 are approximately 0.4 for billboard arrays, 0.25 for 2D nested arrays, 0.35 for OBA, 0.3 for HOBA, 0.45 for HOBA-2, and 0.5 for hourglass arrays. This phenomenon indicates that hourglass arrays are more robust to mutual coupling effects than the others. Fig. 9(b) plots the RMSE versus c_1 if the number of sources $D = 36$. The thresholds of c_1 become 0.15 for billboard arrays, 0.1 for 2D nested arrays, OBA, HOBA, and 0.2 for HOBA-2 and hourglass arrays, since it is more difficult to resolve 36 sources simultaneously than to resolve 9 sources. Note that, even in the extreme case of $D = 36$ and $c_1 = 0.2$, hourglass arrays still enjoy the RMSE as small as 10^{-3}, which is much smaller than those for URA, billboard arrays, 2D nested arrays, OBA, and HOBA.

Note that the number of sources is much smaller than sensors ($9, 36 \ll 81$). It is conjectured that, 2D sparse arrays might resolve more sources than sensors almost surely, in the *absence* of mutual coupling. However, if mutual coupling is present, this is more challenging, and it will be explored in greater detail in future.

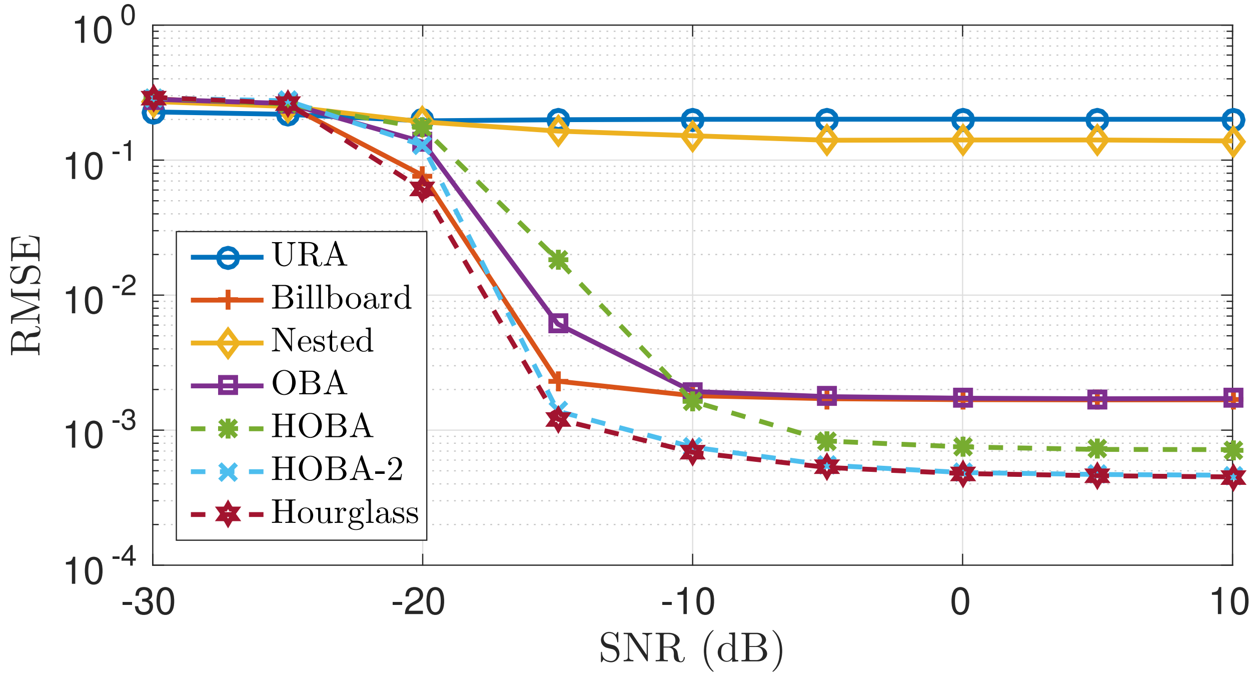

(a)

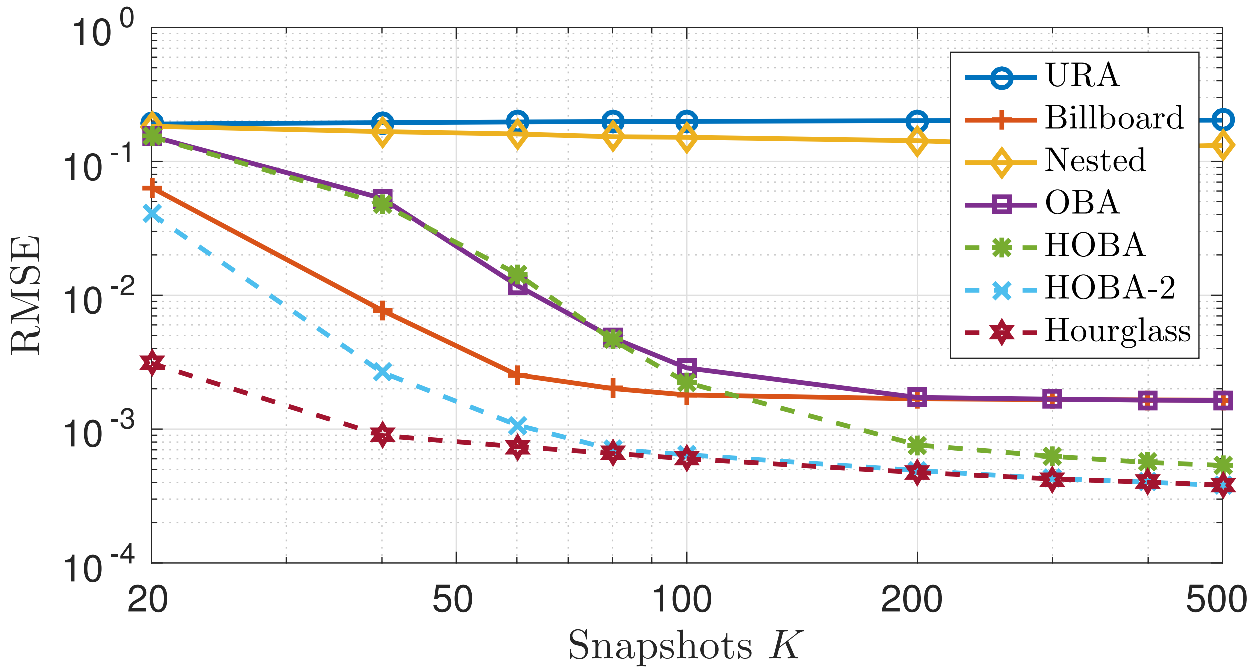

(b)

Fig. 8. The RMSE as a function of (a) SNR and (b) the number of snapshots K. The array geometries are illustrated in [31, Section II]. The number of sensors is 81 for all arrays. The parameters are (a) $K = 200$, the number of sources $D = 9$ and (b) 0dB SNR, $D = 9$. The sources directions are depicted in Fig. 7. Each point is averaged from 1000 runs.

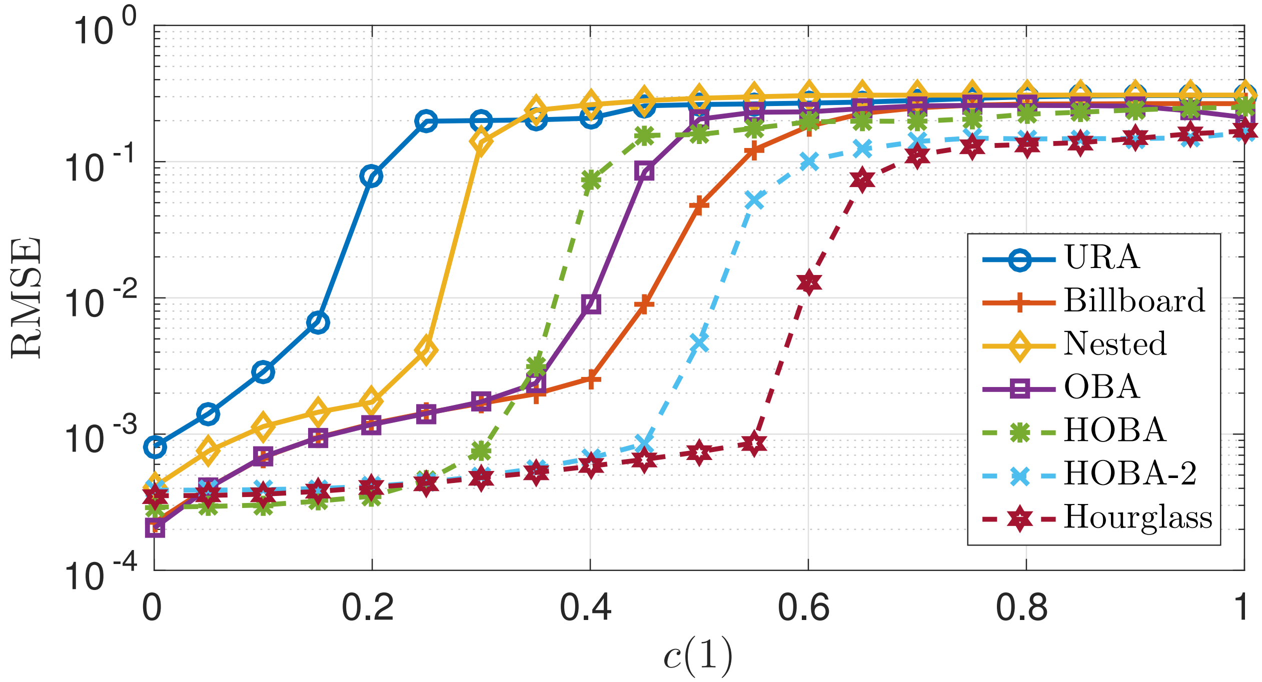

(a)

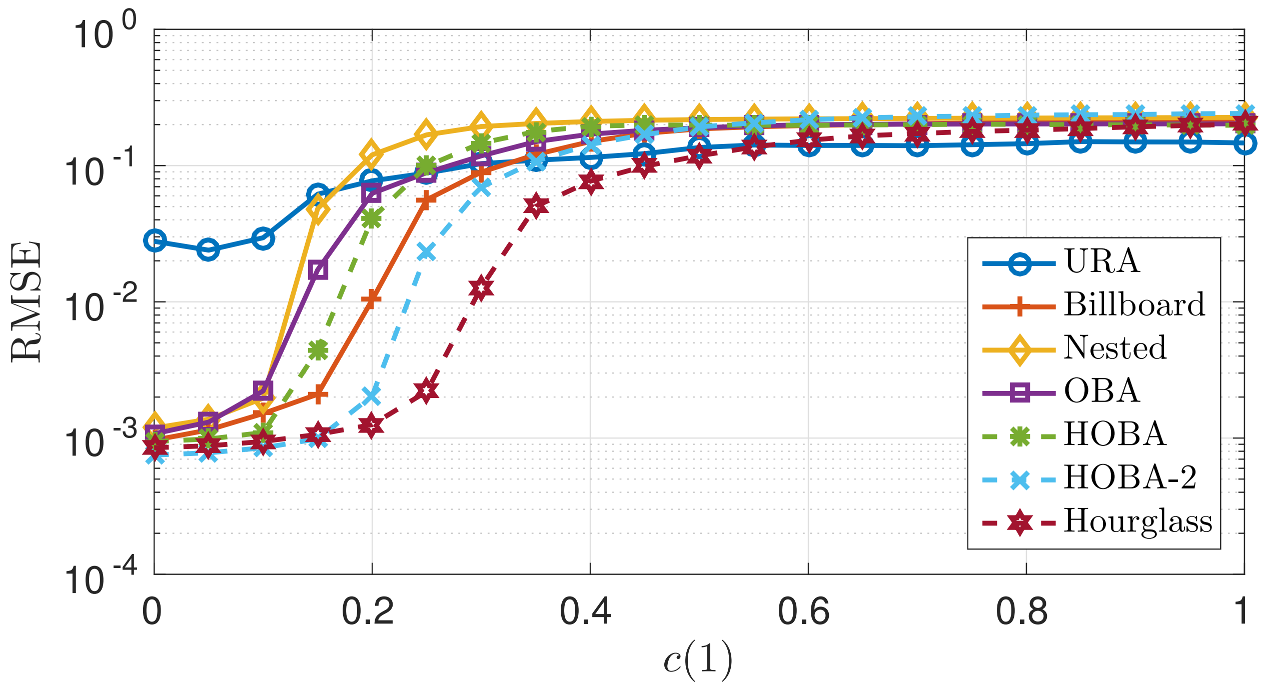

(b)

Fig. 9. The RMSE as a function of the mutual coupling model for (a) the number of sources $D = 9$ and (b) $D = 36$. The array geometries are illustrated in [31, Section II]. The number of sensors is 81 for all arrays. The parameters are 0dB SNR and $K = 200$. The sources directions are depicted in Fig. 7. The mutual coupling model is characterized by $B = 5$ and $c(\ell) = c(1)e^{j\pi(\ell-1)/4}/\ell$. Each point is averaged from 1000 runs.

IX. Concluding Remarks

In this paper, we proposed several generalizations of OBA, including POBA, HOBA, POBA-L, HOBA-2, and hourglass arrays. These arrays enjoy closed-form sensor locations, hole-free coarrays, and reduced mutual coupling effects. Our numerical examples show that, hourglass arrays perform better than the others, in the presence of mutual coupling.

Note that the hourglass array is one of the array configurations that satisfy Theorem 2. In the future, it will be of considerable interest to study the array configurations which not only satisfy Theorem 2 but also own even less mutual coupling than hourglass arrays.

Appendix A
Proof of Lemma 1

The proof can be divided into four cases:

1) If $a_p < 0$, consider the sensor pair in $\mathbb{S}'$: $(N_x - 1, N_y - 1)$ and (a_p, b_p). Their difference is $(N_x - 1 - a_p, N_y - 1 - b_p) \notin \mathbb{D}_{\text{OBA}}$, since the first coordinate $N_x - 1 - a_p > N_x - 1$.
2) If $a_p > N_x - 1$, for the sensor pair $(a_p, b_p), (0, N_y - 1) \in \mathbb{S}'$, the difference becomes $(a_p, b_p - N_y + 1) \notin \mathbb{D}_{\text{OBA}}$ because $a_p > N_x - 1$.
3) If $b_p < 0$, we can take the sensor pair of $(0, N_y - 1)$ and (a_p, b_p). The difference is $(-a_p, N_y - 1 - b_p) \notin \mathbb{D}_{\text{OBA}}$.
4) If $b_p > N_y - 1$, we have the following chain of arguments. Since $P < N_x$, there must exist a element $(n', 0) \in \mathbb{S}'$. Then the difference between (a_p, b_p) and $(n', 0)$ is $(a_p - n', b_p) \notin \mathbb{D}_{\text{OBA}}$, because $b_p > N_y - 1$.

These arguments show that $0 \leq a_p \leq N_x - 1$ and $0 \leq b_p \leq N_y - 1$ are necessary for $\mathbb{D}_{\text{OBA}} = \mathbb{D}'$. Furthermore, since $(a_p, b_p) \notin \mathbb{S}_{\text{OBA}}$, the necessary condition becomes $1 \leq a_p \leq N_x - 2$ and $1 \leq b_p \leq N_y - 1$, which proves this lemma.

Appendix B
Proof of Lemma 2

Assume that $\mathbb{D}_{\text{OBA}} = \mathbb{D}'$. We obtain $(N_x - 1, N_y - 1) \in \mathbb{D}_{\text{OBA}} = \mathbb{D}'$. Due to Lemma 1, the only sensor pair with this separation is $(N_x - 1, N_y - 1)$ and $(0, 0)$, implying $(0, 0) \in \mathbb{S}'$. Similar arguments apply to the sensor pair of $(N_x - 1, 0)$ and $(0, N_y - 1)$, which proves this lemma.

Appendix C
Proof of Theorem 1

Let $\mathbb{S}_{\text{OBA}}$ and $\mathbb{S}_{\text{POBA}}$ be an open box array and a partially open box array, respectively. Their difference coarrays are denoted by $\mathbb{D}_{\text{OBA}}$ and $\mathbb{D}_{\text{POBA}}$. It is clear that $\mathbb{D}_{\text{POBA}} \subseteq \mathbb{D}_{\text{OBA}}$, due to (6) and Lemma 1.

(Sufficiency) We will show that if $\{\mathfrak{g}_1, N_x - 1 - \mathfrak{g}_2\}$ is a partition of $\{1, 2, \ldots, N_x - 2\}$, then $\mathbb{D}_{\text{OBA}} \subseteq \mathbb{D}_{\text{POBA}}$. That is, for every $\mathbf{m} = (m_x, m_y) \in \mathbb{D}_{\text{OBA}}$, there exists at least one sensor pair $(\mathbf{n}_1, \mathbf{n}_2) \in \mathbb{S}_{\text{POBA}}^2$ such that $\mathbf{n}_1 - \mathbf{n}_2 = \mathbf{m}$. Note that we only need to check half of the elements in $\mathbb{D}_{\text{OBA}}$, since weight functions are symmetric, i.e., $w(\mathbf{m}) = w(-\mathbf{m})$ [9]. If $\{\mathfrak{g}_1, N_x - 1 - \mathfrak{g}_2\}$ is a partition of $\{1, 2, \ldots, N_x - 2\}$, then $\{\mathfrak{g}_2, N_x - 1 - \mathfrak{g}_1\}$ is

TABLE III

12 CASES IN THE PROOF OF THEOREM 1

Case	m_x	m_y	$\mathbf{n}_1$	$\mathbf{n}_2$
1	0	0	$(0,0) \in \mathbb{S}_{\text{POBA}}$	$(0,0) \in \mathbb{S}_{\text{POBA}}$
2	$\in \mathfrak{g}_1$		$(m_x, 0) \in \mathbb{G}_1$	$(0,0) \in \mathbb{S}_{\text{POBA}}$
3	$\in N_x - 1 - \mathfrak{g}_2$		$(N_x - 1, N_y - 1) \in \mathbb{S}_{\text{POBA}}$	$(N_x - 1 - m_x, N_y - 1) \in \mathbb{G}_2$
4	$N_x - 1$		$(N_x - 1, 0) \in \mathbb{S}_{\text{POBA}}$	$(0,0) \in \mathbb{S}_{\text{POBA}}$
5	0	$1 \leq m_y \leq N_y - 1$	$(0, m_y) \in \mathbb{S}_{\text{POBA}}$	$(0,0) \in \mathbb{S}_{\text{POBA}}$
6	$\in N_x - 1 - \mathfrak{g}_1$		$(N_x - 1, m_y) \in \mathbb{S}_{\text{POBA}}$	$(N_x - 1 - m_x, 0) \in \mathbb{G}_1$
7	$\in \mathfrak{g}_2$		$(m_x, N_y - 1) \in \mathbb{G}_2$	$(0, N_y - 1 - m_y) \in \mathbb{S}_{\text{POBA}}$
8	$N_x - 1$		$(N_x - 1, m_y) \in \mathbb{S}_{\text{POBA}}$	$(0,0) \in \mathbb{S}_{\text{POBA}}$
9	0	$-N_y + 1 \leq m_y \leq -1$	$(0,0) \in \mathbb{S}_{\text{POBA}}$	$(0, -m_y) \in \mathbb{S}_{\text{POBA}}$
10	$\in \mathfrak{g}_1$		$(m_x, 0) \in \mathbb{G}_1$	$(0, -m_y) \in \mathbb{S}_{\text{POBA}}$
11	$\in N_x - 1 - \mathfrak{g}_2$		$(N_x - 1, N_y - 1 + m_y) \in \mathbb{S}_{\text{POBA}}$	$(N_x - 1 - m_x, N_y - 1) \in \mathbb{G}_2$
12	$N_x - 1$		$(N_x - 1, N_y - 1 + m_y) \in \mathbb{S}_{\text{POBA}}$	$(0, N_y - 1) \in \mathbb{S}_{\text{POBA}}$

also a partition of $\{1, 2, \ldots, N_x - 2\}$. Due to this property, we can identify at least one $(\mathbf{n}_1, \mathbf{n}_2)$ pair for any given difference (m_x, m_y), as listed in Table III, which proves the sufficiency.

(Necessity) If $\{\mathfrak{g}_1, N_x - 1 - \mathfrak{g}_2\}$ is not a partition of $\{1, 2, \ldots, N_x - 2\}$, then $\mathfrak{g}_1 \cup (N_x - 1 - \mathfrak{g}_2) \neq \{1, 2, \ldots, N_x - 2\}$ or $\mathfrak{g}_1$ and $N_x - 1 - \mathfrak{g}_2$ are not disjoint. Now there are two possible cases: For the first case, if $\mathfrak{g}_1 \cup (N_x - 1 - \mathfrak{g}_2) \neq \{1, 2, \ldots, N_x - 2\}$, there must exist $n_0 \in \{1, 2, \ldots, N_x - 2\}$ such that $n_0 \notin \mathfrak{g}_1$ and $n_0 \notin N_x - 1 - \mathfrak{g}_2$, since $\mathfrak{g}_1$ and $\mathfrak{g}_2$ are subsets of $\{1, 2, \ldots, N_x - 2\}$ (the first item in Definition 4). We will show that, $(N_x - 1 - n_0, 1) \notin \mathbb{D}_{\text{POBA}}$.

Suppose there exist $(\mathbf{n}_1, \mathbf{n}_2) \in \mathbb{S}_{\text{POBA}}^2$ such that $\mathbf{n}_1 - \mathbf{n}_2 = (N_x - 1 - n_0, 1)$. This means the y coordinates of $\mathbf{n}_1$ and $\mathbf{n}_2$ must differ by 1. According to Definition 4, there are only two cases of $\mathbf{n}_1$ and $\mathbf{n}_2$:

1) If $\mathbf{n}_1 \in \mathbb{H}_2$ and $\mathbf{n}_2 \in \mathbb{G}_1$, then the difference $(N_x - 1 - n_0, 1)$ is achieved only when $\mathbf{n}_1 = (N_x - 1, 1)$ and $\mathbf{n}_2 = (n_0, 0)$. We have $\mathbf{n}_1 \in \mathbb{H}_2$ but $\mathbf{n}_2 \notin \mathbb{G}_1$, since $n_0 \notin \mathfrak{g}_1$.
2) If $\mathbf{n}_1 \in \mathbb{G}_2$ and $\mathbf{n}_2 \in \mathbb{H}_1$, then $\mathbf{n}_1 = (N_x - 1 - n_0, N_y - 1)$ and $\mathbf{n}_2 = (0, N_y - 2)$. We obtain $\mathbf{n}_1 \notin \mathbb{G}_2$ since $n_0 \notin N_x - 1 - \mathfrak{g}_2$.

For the second case, if $\mathfrak{g}_1$ and $N_x - 1 - \mathfrak{g}_2$ are not disjoint, then the size of $\mathfrak{g}_1 \cup (N_x - 1 - \mathfrak{g}_2)$ can be expressed as

$$
\begin{aligned}
&|\mathfrak{g}_1 \cup (N_x - 1 - \mathfrak{g}_2)| \\
&= |\mathfrak{g}_1| + |N_x - 1 - \mathfrak{g}_2| - |\mathfrak{g}_1 \cap (N_x - 1 - \mathfrak{g}_2)| \\
&< |\mathfrak{g}_1| + |\mathfrak{g}_2| = N_x - 2,
\end{aligned}
$$

which implies $\mathfrak{g}_1 \cup (N_x - 1 - \mathfrak{g}_2) \neq \{1, 2, \ldots, N_x - 2\}$. These arguments complete the proof.

APPENDIX D
PROOF OF THEOREM 2

(Sufficiency) The proof of this theorem is similar to that of Theorem 1. We need to show that, if $\{\mathfrak{h}_{1,\ell}\}_{\ell=1}^{L}$ satisfies (10), then for every $\mathbf{m} = (m_x, m_y) \in \mathbb{D}_{\text{OBA}}$, there exist $\mathbf{n}_1, \mathbf{n}_2 \in \mathbb{S}_{\text{POBA-}L}$ such that $\mathbf{n}_1 - \mathbf{n}_2 = \mathbf{m}$. It

TABLE IV

19 CASES IN THE PROOF OF THEOREM 2

Case	m_x	m_y	$\mathbf{n}_1$	$\mathbf{n}_2$	Remarks
1	0	0	$(0,0) \in \mathbb{S}_{\text{POBA-}L}$	$(0,0) \in \mathbb{S}_{\text{POBA-}L}$	
2	$\in \mathfrak{g}_1$	0	$(m_x, 0) \in \mathbb{G}_1$	$(0,0) \in \mathbb{S}_{\text{POBA-}L}$	$\{\mathfrak{g}_1, N_x - 1 - \mathfrak{g}_2\}$
3	$\in N_x - 1 - \mathfrak{g}_2$	0	$(N_x - 1, N_y - 1) \in \mathbb{S}_{\text{POBA-}L}$	$(N_x - 1 - m_x, N_y - 1) \in \mathbb{G}_2$	partitions $\{1, \dots, N_x - 2\}$
4	$N_x - 1$	0	$(N_x - 1, 0) \in \mathbb{S}_{\text{POBA-}L}$	$(0,0) \in \mathbb{S}_{\text{POBA-}L}$	
5	$-(N_x - 1)$	$N_y - 1$	$(0, N_y - 1) \in \mathbb{S}_{\text{POBA-}L}$	$(N_x - 1, 0) \in \mathbb{S}_{\text{POBA-}L}$	
6	$\in -\mathfrak{g}_1$	$N_y - 1$	$(0, N_y - 1) \in \mathbb{S}_{\text{POBA-}L}$	$(-m_x, 0) \in \mathbb{G}_1$	$\{\mathfrak{g}_1, N_x - 1 - \mathfrak{g}_2\}$
7	$\in -(N_x - 1 - \mathfrak{g}_2)$	$N_y - 1$	$(N_x - 1 + m_x, N_y - 1) \in \mathbb{G}_2$	$(N_x - 1, 0) \in \mathbb{S}_{\text{POBA-}L}$	partitions $\{1, \dots, N_x - 2\}$
8	0	$N_y - 1$	$(0, N_y - 1) \in \mathbb{S}_{\text{POBA-}L}$	$(0,0) \in \mathbb{S}_{\text{POBA-}L}$	
9	$\in N_x - 1 - \mathfrak{g}_1$	$N_y - 1$	$(N_x - 1, N_y - 1) \in \mathbb{S}_{\text{POBA-}L}$	$(N_x - 1 - m_x, 0) \in \mathbb{G}_1$	$\{N_x - 1 - \mathfrak{g}_1, \mathfrak{g}_2\}$
10	$\in \mathfrak{g}_2$	$N_y - 1$	$(m_x, N_y - 1) \in \mathbb{G}_2$	$(0,0) \in \mathbb{S}_{\text{POBA-}L}$	partitions $\{1, \dots, N_x - 2\}$
11	$N_x - 1$	$N_y - 1$	$(N_x - 1, N_y - 1) \in \mathbb{S}_{\text{POBA-}L}$	$(0,0) \in \mathbb{S}_{\text{POBA-}L}$	
12	$0 < m_x < (N_x - 1) - (\ell - 1)$	$\in \mathfrak{h}_{2,\ell}$	$(N_x - \ell, m_y) \in \mathbb{H}_{2,\ell}$	$(N_x - \ell - m_x, 0) \in \mathbb{G}_1$	if $N_x - \ell - m_x \in \mathfrak{g}_1$
13	$0 < m_x < (N_x - 1) - (\ell - 1)$	$\in \mathfrak{h}_{2,\ell}$	$(m_x + \ell - 1, N_y - 1) \in \mathbb{G}_2$	$(\ell - 1, N_y - 1 - m_y) \in \mathbb{H}_{1,\ell}$	if $m_x + \ell - 1 \in \mathfrak{g}_2$
14	$N_x - \ell$	$\in \mathfrak{h}_{2,\ell}$	$(N_x - \ell, m_y) \in \mathbb{H}_{2,\ell}$	$(0,0) \in \mathbb{S}_{\text{POBA-}L}$	
15	$N_x - k$ for $1 \leq k \leq \ell - 1$	$\in \mathfrak{h}_{2,\ell}$	$(N_x - p, m_y + r) \in \mathbb{H}_{2,p}$	$(k - p, r) \in \mathbb{H}_{1,k-p+1}$	if $\exists\, p \in \{1, \dots, k\}$ and $\exists\, r \in \mathfrak{h}_{1,k-p+1}$ such that $m_y + r \in \mathfrak{h}_{2,p}$
16	$-(N_x - 1) + (\ell - 1) < m_x < 0$	$\in \mathfrak{h}_{1,\ell}$	$(\ell - 1, m_y) \in \mathbb{H}_{1,\ell}$	$(\ell - 1 - m_x, 0) \in \mathbb{G}_1$	if $\ell - 1 - m_x \in \mathfrak{g}_1$
17	$-(N_x - 1) + (\ell - 1) < m_x < 0$	$\in \mathfrak{h}_{1,\ell}$	$(N_x - \ell + m_x, N_y - 1) \in \mathbb{G}_2$	$(N_x - \ell, N_y - 1 - m_y) \in \mathbb{H}_{2,\ell}$	if $N_x - \ell + m_x \in \mathfrak{g}_2$
18	$-(N_x - \ell)$	$\in \mathfrak{h}_{1,\ell}$	$(\ell - 1, m_y) \in \mathbb{H}_{1,\ell}$	$(N_x - 1, 0) \in \mathbb{S}_{\text{POBA-}L}$	
19	$-(N_x - k)$ for $1 \leq k \leq \ell - 1$	$\in \mathfrak{h}_{1,\ell}$	$(p - 1, m_y + r) \in \mathbb{H}_{1,p}$	$(N_x - (k - p + 1), r) \in \mathbb{H}_{2,k-p+1}$	if $\exists\, p \in \{1, ..., k\}$ and $\exists\, r \in \mathfrak{h}_{2,k-p+1}$ such that $m_y + r \in \mathfrak{h}_{1,p}$

For Case 12 - 19, the parameter ℓ satisfies $1 \leq \ell \leq L$.

suffices to consider $0 \leq |m_x| \leq N_x - 1$ and $0 \leq m_y \leq N_y - 1$ since the weight functions satisfy $w(\mathbf{m}) = w(-\mathbf{m})$.

For $0 \leq |m_x| \leq N_x - 1$ and $0 \leq m_y \leq N_y - 1$, the associated $\mathbf{n}_1$ and $\mathbf{n}_2$ are summarized into 19 cases in Table IV. In particular, some cases are elaborated as follows:

(Case 6, 7, 9, 10) In Case 6 and 7, since $\{\mathfrak{g}_1, N_x - 1 - \mathfrak{g}_2\}$ is a partition of $\{1, \dots, N_x - 2\}$, for $-(N_x - 1) < m_x < 0$ and $m_y = N_y - 1$, the pair $(\mathbf{n}_1, \mathbf{n}_2)$ can be identified using either Case 6 or 7. Similar arguments can be applied to Case 9 and 10.

(Case 12, 13, 16, 17) For $0 < m_x < (N_x - 1) - (\ell - 1)$ and $0 < m_y < N_y - 1$, it is guaranteed that either Case 12 or 13 can be exploited to identify the sensor pair $\mathbf{n}_1$ and $\mathbf{n}_2$. This is true because $\{\mathfrak{g}_1, N_x - 1 - \mathfrak{g}_2\}$ is a partition of $\{1, \dots, N_x - 2\}$, and $\{\mathfrak{h}_{2,\ell}\}_{\ell=1}^{L}$ is a partition of $\{1, \dots, N_y - 2\}$. Case 16 and 17 are similar to Case 12 and 13.

(Case 15) In this case, for some $p \in \{1, \dots, k\}$, if there exists $r \in \mathfrak{h}_{1,k-p+1}$ such that $m_y + r \in \mathfrak{h}_{2,p}$, then, by definition, it can be deduced that $\mathbf{n}_1 \in \mathbb{H}_{2,p}$ and $\mathbf{n}_2 \in \mathbb{H}_{1,k-p+1}$. This sufficient condition is equivalent to

$$\exists\, r \in \mathfrak{h}_{1,k-p+1},\ \exists\, s \in \mathfrak{h}_{2,p},\ \forall\, m_y \in \mathfrak{h}_{2,\ell},$$

$$\text{such that } m_y + r = s.$$

Letting $\widetilde{s} = N_y - 1 - s$ and $\widetilde{m}_y = N_y - 1 - m_y$ yields

$$\begin{aligned}&\exists\, r \in \mathfrak{h}_{1,k-p+1},\ \exists\, \widetilde{s} \in \mathfrak{h}_{1,p},\ \forall\, \widetilde{m}_y \in \mathfrak{h}_{1,\ell}\\ &\quad\text{such that } \widetilde{m}_y = \widetilde{s} + r.\end{aligned} \tag{26}$$

Eq. (26) indicates that, any element in $\mathfrak{h}_{1,\ell}$ can be expressed as the sum of an element in $\mathfrak{h}_{1,p}$ and an element in $\mathfrak{h}_{1,k-p+1}$. Therefore, we obtain

$$\begin{aligned}\mathfrak{h}_{1,\ell} &\subseteq \mathfrak{h}_{1,p} \oplus \mathfrak{h}_{1,k-p+1} = (\mathfrak{h}_{1,p} \oplus \mathfrak{h}_{1,q})|_{p+q=k+1}\\ &\subseteq \bigcup_{\widetilde{p}+\widetilde{q}=k+1} \mathfrak{h}_{1,\widetilde{p}} \oplus \mathfrak{h}_{1,\widetilde{q}} = \mathbb{P}_{k+1},\end{aligned} \tag{27}$$

where $2 \leq k+1 \leq \ell$. If (10) holds true, then (27) also holds true, and so does (26). Therefore, there exist $\mathbf{n}_1 \in \mathbb{H}_{2,p}$ and $\mathbf{n}_2 \in \mathbb{H}_{1,k-p+1}$ such that $\mathbf{n}_1 - \mathbf{n}_2 = \mathbf{m}$.

(Case 19) The proof of this case is similar to that of Case 15. For some $p \in \{1, \ldots, k\}$, the sufficient condition on the last row of Table IV is equivalent to this statement:

$$\begin{aligned}&\exists\, r \in \mathfrak{h}_{2,k-p+1},\ \exists\, s \in \mathfrak{h}_{1,p},\ \forall\, m_y \in \mathfrak{h}_{1,\ell},\\ &\quad\text{such that } m_y + r = s.\end{aligned}$$

Setting $\widetilde{r} = N_y - 1 - r$ gives

$$\begin{aligned}&\exists\, \widetilde{r} \in \mathfrak{h}_{1,k-p+1},\ \exists\, s \in \mathfrak{h}_{1,p},\ \forall\, m_y \in \mathfrak{h}_{1,\ell}\\ &\quad\text{such that } m_y = s + \widetilde{r} - (N_y - 1).\end{aligned}$$

Similar to (27), we have $\mathfrak{h}_{1,\ell} \subseteq \mathbb{P}_{k+1} - (N_y - 1)$. Hence, if (10) is satisfied, then $\mathbf{n}_1 \in \mathbb{H}_{1,p}$ and $\mathbf{n}_2 \in \mathbb{H}_{2,k-p+1}$.

(Necessity) This part can be proved by contradiction. If there exists $n \in \mathfrak{h}_{1,\ell}$ such that $n \notin \mathbb{P}_{\ell'}$ for some $\ell' \leq \ell$, then $\mathbf{m} = (N_x + 1 - \ell', N_y - 1 - n)$ is a hole in $\mathbb{D}_{\text{POBA-}L}$. We will show that there do not exist any sensor pairs $(\mathbf{n}_1, \mathbf{n}_2) \in \mathbb{S}^2_{\text{POBA-}L}$ such that $\mathbf{n}_1 - \mathbf{n}_2 = (N_x + 1 - \ell', N_y - 1 - n)$. Enumerating all possible combinations of $(\mathbf{n}_1, \mathbf{n}_2)$ leads to the following:

1) If $\mathbf{n}_2 = (0,0)$, then $\mathbf{n}_1 = (N_x - (\ell' - 1), N_y - 1 - n)$. According to the x coordinate of $\mathbf{n}_1$, $\mathbf{n}_1$ could belong to $\mathbb{G}_1$, $\mathbb{H}_{2,\ell'-1}$, or $\mathbb{G}_2$. However, based on the y coordinate of $\mathbf{n}_1$, we have $n \in \mathfrak{h}_{1,\ell}$, and $N_x - 1 - n \in \mathfrak{h}_{2,\ell}$. Furthermore, since $\{\mathfrak{h}_{2,\ell}\}_{\ell=1}^{L}$ is a partition of $\{1, \ldots, N_y - 2\}$, we have $\mathbf{n}_1 \in \mathbb{H}_{2,\ell}$. This is a contradiction.
2) $\mathbf{n}_2 = (N_x - 1, 0), (0, N_y - 1), (N_x - 1, N_y - 1)$ or $\mathbf{n}_2 \in \mathbb{G}_2$. It is evident that $\mathbf{n}_1 = \mathbf{n}_2 + \mathbf{m} \notin \mathbb{S}_{\text{POBA-}L}$.
3) If $\mathbf{n}_2 = (n_x, 0) \in \mathbb{G}_1$, then $\mathbf{n}_1 = (N_x - (\ell' - 1 - n_x), N_y - 1 - n)$. The y coordinate of $\mathbf{n}_1$ indicates that $\mathbf{n}_1$ belongs to $\mathbb{H}_{2,\ell}$. From the x coordinate of $\mathbf{n}_1$, we have $\ell' - 1 - n_x = \ell$. By definition, $\ell' \leq \ell$ and $n_x \geq 1$ suggest that $\ell' - 1 - n_x \leq \ell - 2$, causing a contradiction.
4) If $\mathbf{n}_2 = (p - 1, r) \in \mathbb{H}_{1,p}$, then $\mathbf{n}_1 = (N_x - (\ell' - p), N_y - 1 + r - n)$. The x coordinate of $\mathbf{n}_1$ leads to three cases:

a) If $\mathbf{n}_1 \in \mathbb{G}_1$, then $N_y - 1 + r - n = 0$ so $r = n - (N_y - 1)$. Since $n \in \mathfrak{h}_{1,\ell}$, we have $1 \leq n \leq N_y - 2$ and then $-N_y + 2 \leq r \leq -1$. This statement contradicts with $r \in \mathfrak{h}_{1,p} \subseteq \{1, \ldots, N_y - 2\}$.

b) If $\mathbf{n}_1 \in \mathbb{G}_2$, from the y coordinate of $\mathbf{n}_1$, we obtain $N_y - 1 + r - n = N_y - 1$ so $r = n$. Since $\{\mathfrak{h}_{1,\ell}\}_{\ell=1}^{L}$ is a partition of $\{1, \ldots, N_y - 2\}$, the y coordinate of $\mathbf{n}_2 = (p-1, n)$ implies $\mathbf{n}_2 \in \mathbb{H}_{1,\ell}$. We obtain $p = \ell$. However, the x coordinate of $\mathbf{n}_1$ becomes $N_x - (\ell' - p) = N_x + \ell - \ell' \geq N_x + \ell - \ell = N_x$. Therefore, $\mathbf{n}_1 \notin \mathbb{G}_2$.

c) If $\mathbf{n}_1 \in \mathbb{H}_{2,\ell'-p}$, we obtain $N_y - 1 + r - n \in \mathfrak{h}_{2,\ell'-p}$, which is equivalent to $n - r \in \mathfrak{h}_{1,\ell'-p}$. Since $r \in \mathfrak{h}_{1,p}$, it can be concluded that

$$n \in \mathfrak{h}_{1,\ell'-p} \oplus \mathfrak{h}_{1,p} \subseteq \bigcup_{p+q=\ell'} \mathfrak{h}_{1,p} \oplus \mathfrak{h}_{1,q} = \mathbb{P}_{\ell'},$$

which contradicts with the assumption $n \notin \mathbb{P}_{\ell'}$.

5) If $\mathbf{n}_2 = (N_x - p, r) \in \mathbb{H}_{2,p}$, then $\mathbf{n}_1 = (2N_x + 1 - \ell' - p, N_y - 1 - n + r)$. Since $1 \leq \ell' \leq \ell \leq L$ and $1 \leq p \leq L$, the x coordinate of $\mathbf{n}_1$ ranges from $2N_x - 2L + 1$ to $2N_x - 1$. According to Definition 6, we have $L \leq N_x/2$, so the minimum value of the x coordinate in $\mathbf{n}_1$ is $N_x + 1$, implying $\mathbf{n}_1 \notin \mathbb{S}_{\text{POBA-}L}$.

Second, assume that there exists $n \in \mathfrak{h}_{1,\ell}$ such that $n \notin \mathbb{P}_{\ell'} - (N_y - 1)$ for some $\ell' \leq \ell$. Following the same steps in the previous case, it can be shown that $\mathbf{m} = (N_x + 1 - \ell', -n)$ is a hole in the difference coarray $\mathbb{D}$. As a result, the condition (10) is also necessary.

Appendix E
Proof of Theorem 4

This theorem is a consequence of Theorem 2. We will first show that $\mathfrak{h}_{1,\ell} \subseteq \mathfrak{h}_{1,1} \oplus \mathfrak{h}_{1,\ell'-1} \subseteq \mathbb{P}_{\ell'}$ for every ℓ' and ℓ in $2 \leq \ell' \leq \ell \leq L$. That is, for every $h \in \mathfrak{h}_{1,\ell}$, it suffices to find $n_1 \in \mathfrak{h}_{1,1}$ and $n_2 \in \mathfrak{h}_{1,\ell'-1}$ such that $h = n_1 + n_2$. According to (13), h can be divided into four cases as follows:

(Case 1) If $h = 2\ell - 1$, then n_1 and n_2 are given by

$$n_1 = 2(\ell - \ell' + 1), \qquad n_2 = 2(\ell' - 1) - 1.$$

It can be seen that $n_2 \in \mathfrak{h}_{1,\ell'-1}$. We need to show that $n_1 \in \mathfrak{h}_{1,1}$. Since $2 \leq \ell' \leq \ell \leq L$, we have

$$1 \leq \ell - \ell' + 1 \leq L - 1.$$

The upper bound $L - 1$ can be divided into two cases: If N_y is odd, then $L - 1 = \lfloor (N_y - 3)/4 \rfloor \leq \lfloor (N_y - 1)/4 \rfloor$. If N_y is even, we obtain $L - 1 = \lfloor N_y/8 \rfloor \leq \lfloor (N_y - 1)/4 \rfloor$. In either cases, $n_1 \in \mathfrak{h}_{1,1}$.

(Case 2) If $h = N_y - 2\ell$, it is divided into two cases based on N_y:

1) If N_y is odd, n_1 and n_2 are given by

$$n_1 = N_y - 1 - 2(\ell + \ell' - 2), \;\; n_2 = 2(\ell' - 1) - 1. \tag{28}$$

It is obvious that n_1 is even and $n_2 \in \mathfrak{h}_{1,\ell'-1}$. Next we will prove that $n_1 \in \mathfrak{h}_{1,1}$. since $2 \leq \ell' \leq \ell \leq L$, we have $2 \leq \ell + \ell' - 2 \leq 2L - 2$. There are two subcases according to $\ell + \ell' - 2$:

a) If $2 \leq \ell + \ell' - 2 \leq \lfloor (N_y - 1)/4 \rfloor$, it can be shown that $n_1 \in \mathfrak{h}_{1,1}$.

b) If $\lfloor (N_y - 1)/4 \rfloor + 1 \leq \ell + \ell' - 2 \leq 2L - 2$, then the minimum of n_1 is lower bounded by

$$\begin{aligned} n_{1,\min} &= N_y - 1 - 2(2L - 2) \\ &= 4\left(\frac{N_y + 1}{4} - \left\lfloor \frac{N_y + 1}{4} \right\rfloor\right) + 2 \geq 2. \end{aligned} \tag{29}$$

The maximum of n_1 becomes

$$\begin{aligned} n_{1,\max} &= N_y - 1 - 2(\lfloor (N_y - 1)/4 \rfloor + 1) \\ &= 4 \times \frac{N_y - 1}{4} - 2\left\lfloor \frac{N_y - 1}{4} \right\rfloor - 2. \end{aligned}$$

For odd N_y, it can be shown that $(N_y - 1)/4 \leq \lfloor (N_y - 1)/4 \rfloor + 1/2$. The maximum of n_1 is upper bounded by

$$\begin{aligned} n_{1,\max} &\leq 4\left(\left\lfloor \frac{N_y - 1}{4} \right\rfloor + \frac{1}{2}\right) - 2\left\lfloor \frac{N_y - 1}{4} \right\rfloor - 2 \\ &= 2\left\lfloor \frac{N_y - 1}{4} \right\rfloor. \end{aligned} \tag{30}$$

Hence, $n_1 \in \mathfrak{h}_{1,1}$, due to (13), (29), and (30).

2) If N_y is even, the pair (n_1, n_2) can be written as

$$\begin{aligned} n_1 &= N_y - 2\lceil N_y/4 \rceil - 2(\ell + \ell' - 3), \\ n_2 &= 2\lceil N_y/4 \rceil + 2(\ell' - 1) - 4. \end{aligned}$$

It is also true that $n_2 \in \mathfrak{h}_{1,\ell'-1}$. It suffices to show that $n_1 \in \mathfrak{h}_{1,1}$. Due to even N_y, the qualtity n_1 is even. For $2 \leq \ell' \leq \ell \leq L$, the maximum of n_1 is upper bounded by

$$\begin{aligned} n_{1,\max} &= N_y - 2\lceil N_y/4 \rceil - 2 \leq N_y - 2 \times N_y/4 - 2 \\ &= 2\left(\frac{N_y - 1}{4} - \frac{3}{4}\right) \leq 2\left\lfloor \frac{N_y - 1}{4} \right\rfloor, \end{aligned}$$

where the last inequality is due to $(N_y - 1)/4 - 3/4 \leq \lfloor (N_y - 1)/4 \rfloor$ for even N_y. On the other hand, the minimum of n_1 is given by

$$\begin{aligned} n_{1,\min} &= N_y - 2\lceil N_y/4 \rceil - 2(2L - 3) \\ &= N_y - 2\lceil N_y/4 \rceil - 4\lfloor N_y/8 \rfloor + 2. \end{aligned}$$

Since $N_y/2 = \lfloor N_y/4 \rfloor + \lceil N_y/4 \rceil$ and $\lfloor 2x \rfloor \geq 2\lfloor x \rfloor$, the quantity $n_{1,\min}$ is lower bounded by

$$\begin{aligned} n_{1,\min} &= N_y - 2\left(\frac{N_y}{2} - \left\lfloor \frac{N_y}{4} \right\rfloor\right) - 4\left\lfloor \frac{N_y}{8} \right\rfloor + 2 \\ &\geq 2 \times 2\left\lfloor \frac{N_y}{8} \right\rfloor - 4\left\lfloor \frac{N_y}{8} \right\rfloor + 2 \geq 2. \end{aligned}$$

Therefore, $n_1 \in \mathfrak{h}_{1,1}$ because n_1 is an even number between 2 and $2\lfloor (N_y - 1)/4 \rfloor$.

(Case 3) If N_y is even and $h = 2\lfloor N_y/4 \rfloor - 2\ell + 3$, the pair (n_1, n_2) becomes

$$n_1 = 2\lfloor N_y/4 \rfloor - 2(\ell + \ell') + 6, \qquad n_2 = 2(\ell' - 1) - 1.$$

We will again show that $n_1 \in \mathfrak{h}_{1,1}$. Note that n_1 is an even number. The maximum of n_1 is bounded by

$$n_{1,\max} = 2\lfloor N_y/4 \rfloor - 2 \leq 2\lfloor (N_y-1)/4 \rfloor.$$

The minimum of n_1 is lower bounded by

$$\begin{aligned} n_{1,\min} &= 2\lfloor N_y/4 \rfloor - 2L + 6 = 2\lfloor N_y/4 \rfloor - 2\lfloor N_y/8 \rfloor + 4 \\ &\geq 2\lfloor N_y/4 \rfloor - \lfloor N_y/4 \rfloor + 4 \geq 4. \end{aligned}$$

The inequality is due to $2\lfloor x \rfloor \leq \lfloor 2x \rfloor$. Therefore, $n_1 \in \mathfrak{h}_{1,1}$.

(Case 4) If N_y is even and $h = 2\lceil N_y/4 \rceil + 2\ell - 4$, n_1 and n_2 are given by

$$n_1 = 2(\ell - \ell' + 1), \qquad n_2 = 2\lceil N_y/4 \rceil + 2(\ell' - 1) - 4.$$

The membership of n_1 can be shown as follows: Since $2 \leq \ell' \leq \ell \leq L$, we have

$$1 \leq \ell - \ell' + 1 \leq L - 1 = \lfloor N_y/8 \rfloor \leq \lfloor (N_y-1)/4 \rfloor,$$

so that $n_1 \in \mathfrak{h}_{1,1}$. For n_2, if $\ell' \geq 3$, it is clear that $n_2 \in \mathfrak{h}_{1,\ell'-1}$. If $\ell' = 2$, then n_2 becomes

$$n_2 = 2\lceil N_y/4 \rceil - 2 = 2\lfloor (N_y-1)/4 \rfloor.$$

The last equality can be shown by considering two cases: $N_y = 4r$ and $N_y = 4r + 2$, where r is an integer. Therefore, $n_1 \in \mathfrak{h}_{1,1}$.

So far we have proved the statement that $\mathfrak{h}_{1,\ell} \subseteq \mathbb{P}_{\ell'}$ for $2 \leq \ell' \leq \ell \leq L$. It is required to prove $\mathfrak{h}_{1,\ell} \subseteq \mathbb{P}_{\ell'} - (N_y - 1)$. Based on the definition of $\mathfrak{h}_{1,\ell}$, it is evident that these sets are symmetric. That is, for every $h \in \mathfrak{h}_{1,\ell}$, there uniquely exists $h' \in \mathfrak{h}_{1,\ell}$ such that $h = N_y - 1 - h'$. Since $h' \in \mathfrak{h}_{1,\ell}$, there must exist $n_1' \in \mathfrak{h}_{1,1}$ and $n_2' \in \mathfrak{h}_{1,\ell'-1}$ such that $h' = n_1' + n_2'$. We obtain

$$\begin{aligned} h &= N_y - 1 - h' = N_y - 1 - n_1' - n_2' \\ &= (N_y - 1 - n_1') + (N_y - 1 - n_2') - (N_y - 1). \end{aligned}$$

It can be deduced that $N_y - 1 - n_1' \in \mathfrak{h}_{1,1}$ and $N_y - 1 - n_2' \in \mathfrak{h}_{1,\ell'-1}$, since these sets are symmetric. We have $h \in \mathbb{P}_{\ell'} - (N_y - 1)$, which proves this theorem.

REFERENCES

[1] C.-L. Liu and P. P. Vaidyanathan, "Two-dimensional sparse arrays with hole-free coarray and reduced mutual coupling," in *Proc. IEEE Asil. Conf. on Sig., Sys., and Comp.*, 2016.

[2] H. L. Van Trees, *Optimum Array Processing: Part IV of Detection, Estimation, and Modulation Theory*. Wiley Interscience, 2002.

[3] M. I. Skolnik, *Introduction to Radar Systems*, 3rd ed. McGraw Hill, 2001.

[4] S. Haykin, *Array Signal Processing*. Prentice-Hall, 1984.

[5] B. Friedlander and A. Weiss, "Direction finding in the presence of mutual coupling," *IEEE Trans. Antennas Propag.*, vol. 39, no. 3, pp. 273–284, Mar 1991.

[6] C. A. Balanis, *Antenna Theory: Analysis and Design*, 4th ed. John Wiley & Sons, 2016.

[7] C.-L. Liu and P. P. Vaidyanathan, "Super nested arrays: Linear sparse arrays with reduced mutual coupling–Part I: Fundamentals," *IEEE Trans. Signal Process.*, vol. 64, no. 15, pp. 3997–4012, Aug 2016.

[8] A. T. Moffet, "Minimum-redundancy linear arrays," *IEEE Trans. Antennas Propag.*, vol. 16, no. 2, pp. 172–175, 1968.

[9] P. Pal and P. P. Vaidyanathan, "Nested arrays: A novel approach to array processing with enhanced degrees of freedom," *IEEE Trans. Signal Process.*, vol. 58, no. 8, pp. 4167–4181, Aug 2010.

[10] P. P. Vaidyanathan and P. Pal, "Sparse sensing with co-prime samplers and arrays," *IEEE Trans. Signal Process.*, vol. 59, no. 2, pp. 573–586, Feb 2011.

[11] C.-L. Liu and P. P. Vaidyanathan, "Super nested arrays: Linear sparse arrays with reduced mutual coupling–Part II: High-order extensions," *IEEE Trans. Signal Process.*, vol. 64, no. 16, pp. 4203–4217, Aug 2016.

[12] K. Adhikari, J. R. Buck, and K. E. Wage, "Extending coprime sensor arrays to achieve the peak side lobe height of a full uniform linear array," *EURASIP J. Adv. Signal Process.*, vol. 2014, no. 1, 2014.

[13] S. Qin, Y. Zhang, and M. Amin, "Generalized coprime array configurations for direction-of-arrival estimation," *IEEE Trans. Signal Process.*, vol. 63, no. 6, pp. 1377–1390, March 2015.

[14] Q. Shen, W. Liu, W. Cui, and S. Wu, "Extension of co-prime arrays based on the fourth-order difference co-array concept," *IEEE Signal Process. Lett.*, vol. 23, no. 5, pp. 615–619, May 2016.

[15] P. Pal and P. P. Vaidyanathan, "Nested arrays in two dimensions, Part II: Application in two dimensional array processing," *IEEE Trans. Signal Process.*, vol. 60, no. 9, pp. 4706–4718, Sept 2012.

[16] T. Jiang, N. D. Sidiropoulos, and J. M. F. ten Berge, "Almost-sure identifiability of multidimensional harmonic retrieval," *IEEE Trans. Signal Process.*, vol. 49, no. 9, pp. 1849–1859, Sep 2001.

[17] R. A. Haubrich, "Array design," *Seismol. Soc. Am., Bull.*, vol. 58, no. 3, pp. 977–991, June 1968.

[18] R. Hoctor and S. Kassam, "The unifying role of the coarray in aperture synthesis for coherent and incoherent imaging," *Proc. IEEE*, vol. 78, no. 4, pp. 735–752, Apr 1990.

[19] A. Manikas, *Differential Geometry In Array Processing*. Imperial College Press, 2004.

[20] P. P. Vaidyanathan and P. Pal, "Direct-MUSIC on sparse arrays," in *2012 International Conference on Signal Processing and Communications (SPCOM)*, July 2012.

[21] P. Pal and P. P. Vaidyanathan, "Coprime sampling and the MUSIC algorithm," in *Proc. IEEE Dig. Signal Proc. Signal Proc. Educ. Workshop*, Jan 2011, pp. 289–294.

[22] Z. Tan, Y. Eldar, and A. Nehorai, "Direction of arrival estimation using co-prime arrays: A super resolution viewpoint," *IEEE Trans. Signal Process.*, vol. 62, no. 21, pp. 5565–5576, Nov 2014.

[23] C. R. Greene and R. C. Wood, "Sparse array performance," *J. Acoust. Soc. Am.*, vol. 63, no. 6, pp. 1866–1872, 1978.

[24] P. Pal and P. P. Vaidyanathan, "Nested arrays in two dimensions, Part I: Geometrical considerations," *IEEE Trans. Signal Process.*, vol. 60, no. 9, pp. 4694–4705, Sept 2012.

[25] http://systems.caltech.edu/dsp/students/clliu/Hourglass/Hourglass.zip.

[26] W.-K. Ma, T.-H. Hsieh, and C.-Y. Chi, "DOA estimation of quasi-stationary signals with less sensors than sources and unknown spatial noise covariance: A Khatri-Rao subspace approach," *IEEE Trans. Signal Process.*, vol. 58, no. 4, pp. 2168–2180, April 2010.

[27] C.-L. Liu and P. P. Vaidyanathan, "Remarks on the spatial smoothing step in coarray MUSIC," *IEEE Signal Process. Lett.*, vol. 22, no. 9, pp. 1438–1442, Sept 2015.

[28] T. Svantesson, "Modeling and estimation of mutual coupling in a uniform linear array of dipoles," in *Proc. IEEE Int. Conf. Acoust., Speech, and Sig. Proc.*, vol. 5, 1999, pp. 2961–2964.

[29] ——, "Mutual coupling compensation using subspace fitting," in *Proc. IEEE Sensor Array and Multichannel Signal Processing Workshop*, 2000, pp. 494–498.

[30] E. BouDaher, F. Ahmad, M. G. Amin, and A. Hoorfar, "Mutual coupling effect and compensation in non-uniform arrays for direction-of-arrival estimation," *Digital Signal Processing*, vol. 61, pp. 3–14, 2017, Special Issue on Coprime Sampling and Arrays. [Online]. Available: http://www.sciencedirect.com/science/article/pii/S1051200416300689

[31] http://systems.caltech.edu/dsp/students/clliu/Hourglass/Supp.pdf.

[32] M. D. Zoltowski, M. Haardt, and C. P. Mathews, "Closed-form 2-D angle estimation with rectangular arrays in element space or beamspace via unitary ESPRIT," *IEEE Trans. Signal Process.*, vol. 44, no. 2, pp. 316–328, Feb 1996.

Chun-Lin Liu (S'12) was born in Yunlin, Taiwan, on April 28, 1988. He received the B.S. and M.S. degrees in electrical engineering and communication engineering from National Taiwan University (NTU), Taipei, Taiwan, in 2010 and 2012, respectively. He is currently pursuing the Ph.D. degree in electrical engineering at the California Institute of Technology (Caltech), Pasadena, CA. His research interests are in sparse array signal processing, sparse array design, tensor signal processing, and filter bank design.

He received the Best Student Paper Awards at the 41st IEEE International Conference on Acoustics, Speech and Signal Processing, 2016, Shanghai, China, and the 9th IEEE Sensor Array and Multichannel Signal Processing Workshop, 2016, Rio de Janeiro, Brazil. He was also one of the recipients of the Student Paper Award at the 50th Asilomar Conference on Signals, Systems, and Computers, 2016, Pacific Grove, CA.

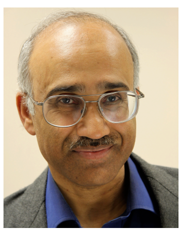

P. P. Vaidyanathan (S'80–M'83–SM'88–F'91) was born in Calcutta, India on Oct. 16, 1954. He received the B.Sc. (Hons.) degree in physics and the B.Tech. and M.Tech. degrees in radiophysics and electronics, all from the University of Calcutta, India, in 1974, 1977 and 1979, respectively, and the Ph.D degree in electrical and computer engineering from the University of California at Santa Barbara in 1982. He was a post doctoral fellow at the University of California, Santa Barbara from Sept. 1982 to March 1983. In March 1983 he joined the electrical engineering department of the Calfornia Institute of Technology as an Assistant Professor, and since 1993 has been Professor of electrical engineering there. His main research interests are in digital signal processing, multirate systems, wavelet transforms, signal processing for digital communications, genomic signal processing, radar signal processing, and sparse array signal processing.

Dr. Vaidyanathan served as Vice-Chairman of the Technical Program committee for the 1983 IEEE International symposium on Circuits and Systems, and as the Technical Program Chairman for the 1992 IEEE International symposium on Circuits and Systems. He was an Associate editor for the IEEE Transactions on Circuits and Systems for the period 1985-1987, and is currently an associate editor for the journal IEEE Signal Processing letters, and a consulting editor for the journal Applied and computational harmonic analysis. He has been a guest editor in 1998 for special issues of the IEEE Trans. on Signal Processing and the IEEE Trans. on Circuits and Systems II, on the topics of filter banks, wavelets and subband coders.

Dr. Vaidyanathan has authored nearly 500 papers in journals and conferences, and is the author/coauthor of the four books Multirate systems and filter banks, Prentice Hall, 1993, Linear Prediction Theory, Morgan and Claypool, 2008, and (with Phoong and Lin) Signal Processing and Optimization for Transceiver Systems, Cambridge University Press, 2010, and Filter Bank Transceivers for OFDM and DMT Systems, Cambridge University Press, 2010. He has written several chapters for various signal processing handbooks. He was a recipient of the Award for excellence in teaching at the California Institute of Technology for the years 1983-1984, 1992-93 and 1993-94. He also received the NSF's Presidential Young Investigator award in 1986. In 1989 he received the IEEE ASSP Senior Award for his paper on multirate perfect-reconstruction filter banks. In 1990 he was recepient of the S. K. Mitra Memorial Award from the Institute of Electronics and Telecommuncations Engineers, India, for his joint paper in the IETE journal. In 2009 he was chosen to receive the IETE students' journal award for his tutorial paper in the IETE Journal of Education. He was also the coauthor of a paper on linear-phase perfect reconstruction filter banks in the IEEE SP Transactions, for which the first author (Truong Nguyen) received the Young outstanding author award in 1993. Dr. Vaidyanathan was elected Fellow of the IEEE in 1991. He received the 1995 F. E. Terman Award of the American Society for Engineering Education, sponsored by Hewlett Packard Co., for his contributions to engineering education. He has given several plenary talks including at the IEEE ISCAS-04, Sampta-01, Eusipco-98, SPCOM-95, and Asilomar-88 conferences on signal processing. He has been chosen a distinguished lecturer for the IEEE Signal Processing Society for the year 1996-97. In 1999 he was chosen to receive the IEEE CAS Society's Golden Jubilee Medal. He is a recepient of the IEEE Signal Processing Society's Technical Achievement Award for the year 2002, and the IEEE Signal Processing Society's Education Award for the year 2012. He is a recipient of the IEEE Gustav Kirchhoff Award (an IEEE Technical Field Award) in 2016, for "Fundamental contributions to digital signal processing." In 2016 he received the Northrup Grumman Prize for excellence in Teaching at Caltech. He is also the recipient of the 2016 Society Award of the IEEE Signal Processing Society.